Journal of
Marine Science and Engineering

MDPI

Review

An Interface Parametric Evaluation on Wellbore Integrity during Natural Gas Hydrate Production

Miaozi Zheng [1], Renjie Yang [2], Jianmin Zhang [1], Yongkai Liu [2], Songlin Gao [2] and Menglan Duan [2,*]

[1] State Key Laboratory of Hydroscience and Engineering, Department of Hydraulic Engineering, Tsinghua University, Beijing 100084, China
[2] College of Safety and Ocean Engineering, China University of Petroleum, Beijing 102249, China
* Correspondence: mlduan@cup.edu.cn

Abstract: Based on the whole life cycle process of the economic exploitation of natural gas hydrate, this paper proposes the basic problem of stabilizing the wellbore for the basic conditions that must be met to ensure the integrity of the wellbore for exploitation: revealing the complex mechanism of fluid–solid–heat coupling in the process of the physical exchange of equilibrium among gas, water, and multiphase sand flows in the wellbore, hydrate reservoir, and wellbore, defining the interface conditions to ensure wellbore stability during the entire life cycle of hydrate production and proposing a scientific evaluation system of interface parameters for wellbore integrity.

Keywords: natural gas hydrate; wellbore stabilization; sand production

Citation: Zheng, M.; Yang, R.; Zhang, J.; Liu, Y.; Gao, S.; Duan, M. An Interface Parametric Evaluation on Wellbore Integrity during Natural Gas Hydrate Production. *J. Mar. Sci. Eng.* **2022**, *10*, 1524. https://doi.org/10.3390/jmse10101524

Academic Editor: Timothy S. Collett

Received: 31 July 2022
Accepted: 6 October 2022
Published: 18 October 2022

1. Introduction

In 2020, the Chinese government proposed to achieve the goal of "carbon peak" by 2030 and "carbon neutrality" by 2060. Currently, China is still in the stage of rapid development of production and construction, with carbon dioxide emissions exceeding 11.9 billion tons in 2021. Among them, the carbon emission of the energy industry accounts for more than 73%. To achieve the carbon peaking and carbon neutrality goals, the energy industry needs to accelerate its entry into a low-carbon transition period. China is limited by the fossil-based energy system and the current state of energy resources. Building an energy system with renewable energy and new energy as the main body effectively achieves the "dual carbon" goal. However, due to its shortcomings, it is difficult for new energy to replace the main position of fossil energy in the short term. To ensure national energy security and stable economic development, increasing the proportion of low-carbon fossil energy natural gas in fossil energy consumption is a reliable way for China to achieve carbon peaking and carbon neutrality safely, stably, and effectively [1,2]. With the increasing depletion of conventional natural gas resources available on land, developing unconventional natural gas resources, especially deep-sea marine energy resources, is significant for developing marine undertakings and maintaining national security rights and interests. Deep-sea shallow strata contain abundant natural gas hydrate resources. Natural gas hydrate is mainly a solid substance with a cage-like crystal structure formed by methane and water molecules. The formation conditions of its low temperature and high pressure also determine that it generally only exists in the permafrost on land or deep seabed strata. Hydrates have the characteristics of high energy density, wide distribution, and large reserves, and are a kind of clean energy with excellent development prospects [3]. The current global distribution of natural gas hydrates is shown in Figure 1.

Gas hydrate is the most widely distributed (more than 50%) form of organic carbon worldwide. It is estimated that the global carbon storage in the natural gas hydrate is 18,000 GT and the volume converted into methane gas is three trillion cubic meters, equivalent to more than twice the total carbon content of conventional fossil fuels proven in the world [4]. Natural gas hydrate is not only clean energy in the future but also

acts as a form of carbon sequestration to effectively suppress environmental problems such as climate warming. Therefore, the research on the exploration and development of natural gas hydrate is not only an effective way to solve the energy shortage but also exploration to establish an economical, efficient, and environmentally friendly society. Since the early 1980s, the major resource countries, including China, have included the development and utilization of natural gas hydrates in their national development plans and have successively invested in resource surveys and research on mining technologies [5]. Since the Soviet Union developed the hydrate resources in the Maisoyaha oil and gas field in 1969, Canada, the United States, Japan, and other countries have also successively carried out hydrate test production experiments. In 2012, the United States conducted a hydrate test mining experiment on the northern slope of Alaska using the CO_2 replacement method. In 2013 and 2017, Japan successfully realized the test mining of submarine hydrates in the Nankai Trough twice. As early as 1999, China launched a particular project for the investigation and research of hydrate resources. In 2017, completing the first trial production of natural gas hydrate in the Shenhu area of the South China Sea marked a significant achievement in China's deep-sea entry, exploration, and development. In 2020, based on the first trial production, the second trial production of natural gas hydrate was completed in the Shenhu waters of the South China Sea, accumulating valuable experience for the commercial production of hydrate (see Figure 2) [6].

Figure 1. Natural gas hydrate distribution around the world [This figure was modified with permission from ref. [7]. Copyright 2009, Elsevier].

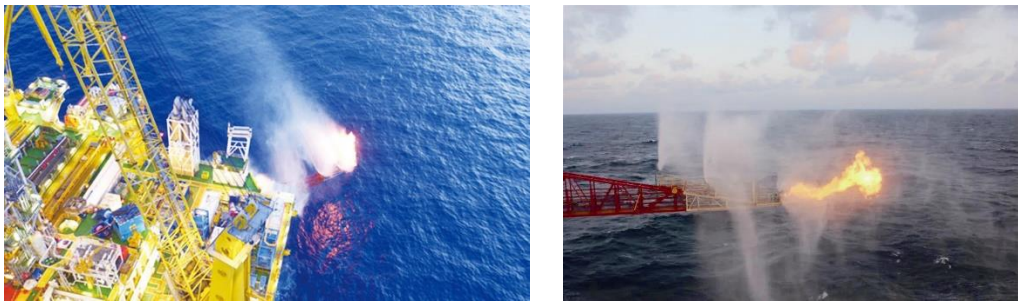

(**a**) (**b**)

Figure 2. Trial production of natural gas hydrate in China. (**a**) The first round of natural gas hydrate trial production in 2017; (**b**) The second round of natural gas hydrate trial production in 2020.

Sand plugging and subsidence collapse are bottleneck problems restricting hydrate production (see Figure 3). Although the test mining process of hydrate is constantly

breaking through, and the results are very gratifying, the sustainable mining of hydrate is still a global problem, and there is still a certain distance from commercial mining. The main reason is that the integrity of the wellbore cannot be effectively guaranteed in the process of hydrate extraction. Sand plugging, subsidence, and collapse significantly damage the integrity of the wellbore, resulting in fatigue in the later stage of hydrate extraction and even production stoppage. Whether it is traditional depressurization, heat injection, chemical inhibitor injection, or relatively cutting-edge CO_2 replacement, the essence is to destroy the phase equilibrium state of the hydrate, promote the phase transition and decomposition of the natural gas hydrate, and then produce natural gas [8–13]. As the hydrate decomposes, its volume rapidly expands hundreds of times, reducing the effective stress of the formation. At the same time, the phase transition process decomposes the hydrates originally belonging to the solid skeleton into gas and liquid, which weakens the cementation of formation particles and reduces the bearing capacity. All these factors make the hydrate-bearing soil subside significantly, seriously damaging the formation's stability and bringing considerable risks to the drilling and production process. In addition, natural gas hydrate mining produces sand easily, resulting in wellbore silting [14]. The two-test production of natural gas hydrate in Japan encountered serious sand production problems, which led to the suspension of the test production. In the process of trial production of natural gas hydrate in the Shenhu area of the South China Sea, the innovative combination of bypass pipe technology and pre-packed screen technology has effectively solved the problem of sand production in the trial production stage, but the short production time still needs further inspection. Other international production tests were forced to suspend, due to the problem of sand production and the failure of long-term stable production. Therefore, to ensure the safe and efficient commercial exploitation of natural gas hydrate, it is necessary to ensure the integrity of the wellbore during the exploitation process, and the problems of sand blocking and subsidence must be effectively dealt with.

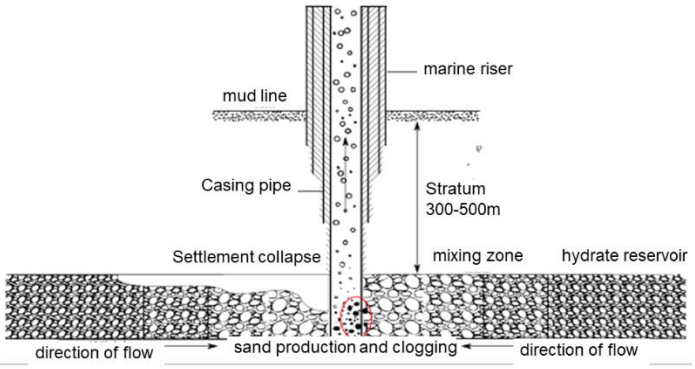

Figure 3. Several typical wellbore integrity failure modes in hydrate production: reservoir subsidence, collapse, and sand production plugging [This figure was modified with permission from ref. [15]. Copyright 2019, Elsevier].

In the wellbore integrity analysis of gas hydrate production, the wellbore and surrounding soil are unified as a whole. While the interface between the wellbore and the soil is generally low in cementation strength, the deformation capacity of the wellbore and the soil is significantly different, which leads to stress concentration or even discontinuous shear deformation at the interface between the two. Therefore, the interface is one of the most critical parts to control wellbore integrity and safety. For gas hydrate extraction, sand production and hydrate decomposition occur on the soil side of the interface, accompanied by complex multi-process coupling, which makes the mechanical behavior of the interface more complicated. However, in the existing wellbore integrity analysis, these characteristics of the interface are not considered, which makes the accuracy of the analysis results and the reliability of the wellbore integrity assessment questionable. To solve these problems, it is necessary to establish the integrated wellbore integrity analysis theory of the deep-sea soil

and mining wells collaborative working system and to analyze all of the deep-sea soil–gas hydrate mining wells in a unified manner.

In the process of integrated wellbore integrity analysis of deep-sea soil and mining well collaborative working system, three issues need to be specifically studied: the mechanical behavior of hydrated soil, the interface characteristics between hydrated soil and mining well, and the hydrate-containing soil–mining well structure interaction. This paper will research on the last two issues including the interface characteristics and structure interaction.

In the process of natural gas hydrate production, the phase transition decomposition and sand production of hydrate will weaken the interface, leading to the failure of wellbore integrity. This interaction is different from the conventional interface. The interaction between the hydrate-containing soil and the production well interface is a multi-process coupling, which includes not only the changes in the temperature field and seepage field of the reservoir caused by the hydrate decomposition process but also the soil deformation and softening, reservoir sand production, multiphase flow process in the wellbore, etc. Therefore, it is necessary to reveal the influence of hydrate decomposition on the mechanical interface behavior, to study the interface weakening mechanism and mathematical description under phase transition conditions, to establish a soil–structure interaction model with phase transition conditions, to develop multi-scale and refined simulation technology for soil–mining well interface considering multi-process coupling and macro and meso-fabric evolution laws and to prove failure mode of natural gas hydrate production under disturbance. The above points are helpful to the establishment of a theoretical system of wellbore integrity evaluation in the process of hydrate production.

2. Soil–Structure Interface Properties

Due to the apparent difference in deformation capacity between soil and wellbore, stress concentration or even large discontinuous shear deformation occurs at the interface between deep-sea soil and gas hydrate production well, which is often a soft surface in the cooperative working system of soil and wellbore. The interaction analysis between soil and structure is essential in studying structural damage. Although the overall analysis of soil and structure can simulate structural damage more accurately, engineering analysis is faced with the following issues: (1) the contact geometry between soil and structure is complex; (2) the mechanical properties of contact between soil and structure are complex; and (3) the scale span between soil and structure is large, and it is difficult to divide the computational grid finely. Therefore, studying the mechanical behavior and the weakening law of the interface between soil and structure is crucial to wellbore integrity. Many scholars have systematically researched the interface between soil and structure, including testing technology, mechanical response and deformation mechanism, and constitutive model.

(1) testing technology

The mechanical properties of the interface between soil and structure refer to the mechanical response law of the interface under the action of monotonic and cyclic shear, mainly including tangential deformation, normal deformation, and strength characteristics. The static and dynamic characteristics of the soil–structure interface are a crucial part of the soil–structure interaction analysis because the deformation and strength characteristics of the soil and the structure on both sides of the interface are very different. Stress concentration and discontinuous deformation occur, which are the weak points of the soil–structure interaction system [16]. Experiments and observations are the basic ways to understand and reveal the mechanical properties, laws and mechanisms of interfaces, are the important means of parameter determination in theoretical models and numerical calculations, and are the only standard to test and verify models and calculation results [17]. Therefore, developing test equipment and related technologies that can simulate the mechanical properties of soil and structure interfaces has received widespread attention. Many scholars have developed and improved the instruments and methods of soil and interface tests and conducted systematic experimental research on mechanical interface properties [18–21].

For the conventional interface shear test, the direct shear tester is the leading piece of equipment for the interface test, some modified from other testing machines and some specially developed to study the mechanical properties of the interface. Desai [22] et al. developed a multi-degree-of-freedom cyclic shearing instrument; Evgin and Fakharian [23] developed a cyclic three-dimensional interface shearing instrument, which can perform two types of tests, direct shearing and single shearing, and can perform shearing on a plane; Gao Jun he [24] and others developed a large-scale single-shear instrument that can perform interface tests. Wangjia Quan et al. have developed a large-scale visual direct shear test instrument suitable for various working conditions, which realizes the front view of direct shear test and automatic collection of test data and can carry out direct shearing of different geosynthetic materials and soil tests [25]. However, most of these test facilities are not adequate considering the characteristics of the interface itself, leading to the inaccuracy of the test: the actual application of normal stress is the soil body rather than the interface itself, which makes it difficult to control the normal boundary conditions of the interface and the error of measuring the normal stress. It is limited to observing its shear characteristics and ignoring the normal deformation and the coupling characteristics of the normal stress–strain relationship and the tangential stress–strain relationship. Zhang Ga and Zhang Jianmin [26] considered the above characteristics and developed a large-scale soil–structure interface cyclic loading shear instrument, which can better simulate and reproduce the physical and mechanical properties and evolution law of the coarse-grained soil–structure interface under monotonic and cyclic loading. Xu Hanqiang et al. developed a large-scale direct shear device considering the temperature effect by adding a constant temperature heating system to the direct shear device, which can be used to study the interaction between different pile materials and soil under the coupling action of temperature and external load [27]. Abdel Salam et al. corrected the equipment and test procedure for the traditional borehole shear test to directly measure the t–z curve of the soil–pile interface of the vertically loaded pile [28]. Jakob Vogelsang et al. designed large-scale test rigs for soil–structure interaction experiments that can measure the distribution of shear and normal stress and well displacement, use digital image correlation (DIC) to assess soil deformation, verify soil contact formulations and the constitutive equation [29]. Hisham T. Eid measured peak and residual interfacial shear strength of normally consolidated soils by using a torsional ring shear instrument adapted for soil and interface testing under undrained conditions [30]. Yue Liang et al. developed a method to study the mechanical properties of the steel–soil interface under reciprocating shear conditions and can perform large-scale direct shear experiments under constant stress boundary and constant stiffness boundary conditions, respectively [31].

In order to meet the needs of practical engineering and research, many scholars have further improved the test equipment, which can not only apply constant stress, constant displacement, and constant stiffness conditions in the normal direction but also control the stress and displacement in the tangential direction. At the same time, given the diversity of soil materials and structural panels in practical engineering, the research objects of the interface have been extended from the interface of clay, sand, coarse-grained soil and steel plate, concrete plate, etc., to the interface between special soil and structure [32,33]; at the same time, a series of studies have been carried out on the effects of soil density, water content, and the type and roughness of structural panels on the mechanical interface response [34–36]. While transforming and developing the direct shear test equipment, the corresponding measurement techniques and means have also been improved and updated to observe more mesoscopic phenomena [37].

In the current interfacial shear test research, the microstructure of the soil samples involved is relatively stable. The phase transition and decomposition of hydrates will cause skeleton decomposition and, at the same time, cause changes in temperature and pore pressure, which significantly impact the interface's mechanical properties. The existing interface shear test equipment generally cannot control and monitor the test sample's temperature and pressure field. To study the mechanical properties of the interface between

the hydrate-containing soil and the wellbore, it is necessary to develop an interface shearing device that can precisely control the temperature and pressure to realize the hydrate phase transition.

(2) Mechanical Response and Deformation Mechanism

Regarding the mechanical properties of the soil–structure interface, Clough and Duncan first proposed a hyperbolic relationship between the average shear stress and the relative tangential displacement at the interface between sand and concrete based on experimental results, which was later widely used [38]. Brandt [39] believed that the failure of the interface follows the rigid–plastic shear failure mode. Desai [40] analyzed the relationship between the interface tangential stress and displacement during the loading–unloading–reloading process through the Ottawa sand–concrete slab interface cyclic direct shear experiment. It is found that when the tangential stress reaches its peak value and undergoes a certain cyclic shearing, the relationship between tangential stress and displacement may become a closed curve; the tangential stiffness of the interface increases with the increase in the normal stress, and the number of cycles, and the tangential stress of the interface increases. It is a function of tangential displacement and is affected by normal stress, cycle times, and soil density. Zeghal and Edil [41] pointed out that the interface tangential stress–strain relationship is significantly affected by particle breakage.

The ultimate shear resistance of the interface during the shearing process is the earliest interface mechanical property studied. In the past, scholars mainly focused their research on its influencing factors, such as structural panel roughness, soil moisture content, normal stress, shear rate, cycle times, etc. For different types of interfaces, the main influencing factors are also different. Potyond [20] conducted a relatively systematic direct shear experimental study on the interface of sand, clay, and their mixtures with steel plates, concrete plates, and wood boards and revealed that the strength of the interface between clay and structure could be described by the Mohr–Coulomb strength criterion, including that cohesion and normal stress are related to the two parts. It is found that soil moisture content, panel roughness, soil composition, and normal stress have a significant influence on the interface surface friction. Tsubakihara and Kishida [42] found that there is a critical roughness through the interface experiment of normally consolidated Kawasaki clay and steel plate, and based on this, the interface is divided into three failure modes: relative slip, failure in soil, and joint action of the two modes. When the roughness of the steel plate is greater than the critical roughness, the interface strength is similar to the strength of the clay itself, and the interface failure occurs in the clay; when the roughness of the steel plate is less than the critical roughness, the interface strength is lower than that of the clay. Tsubakihara and Kishida also found that the loading rate has a more significant effect on the peak interface strength but less on the residual strength; the interface strength expressed in the form of effective stress has nothing to do with consolidation pressure and drainage conditions. Zhang Ga [43] believed that the shear strength of the interface between coarse-grained soil and the structure under cyclic loading is basically the same as that under monotonic shearing, independent of the shearing direction, and related to soil properties, normal stress, panel roughness, etc., based on a more systematic two-dimensional interface experiment. Hou Wenjun [44] conducted three-dimensional direct shear experiments on the interface between coarse-grained soil and the structure and showed that the interface shear strength is not significantly affected by the shear path and has a linear relationship with the normal stress, which the Mohr–Coulomb criterion can describe.

The study of mechanical interface properties should comprehensively consider its tangential and normal mechanical responses and the coupling effect of the two directions. Peterson et al. [45] observed apparent shear dilatation in the shear experiment at the interface between dense sand and concrete and steel plate. In the interface experiment formed by sands with different densities, Boulon [46] found that this kind of interface is in the shearing process, large volume deformations occur, and the deformations are concentrated in thin soil layers near the structural panels. Hryciw and Irsyam [47] also observed a similar phenomenon and called this part of the area a shear band; at the same time, they found

that the shear band phenomenon at the interface between dense sand and rough steel plate is pronounced, but there is no obvious shear band at the smooth interface. Hu Liming [40] believed that the thickness of the shear band was about five~six times the average particle size through the photomicroscopic measurement technique. The research of Fakharian [48] shows that the tangential stress–strain relationship of the interface is affected by its volume change; for the smooth structural panel, the interface exhibits shrinkage; for the rough one, the interface shrinks first, and then developed obviously dilation Gómez [49] found that the volume changes are not significant once the interface reaches the residual strength. Zhang Ga and Zhang Jianmin [50] pointed out based on the interface cyclic shearing experiment that under the condition of two-dimensional cyclic shearing, the volume change of the coarse-grained soil and the structure interface can be decomposed into two components: reversible and irreversible, and the two follow different laws. The reversible shear volume change can be further decomposed into isotropic and anisotropic components, and the irreversible shear volume change can be used as a measure of the interface state evolution. Wenjun Hou [44], based on the three-dimensional experiment of the interface between coarse-grained soil and structure, believed that the development law of the irreversible shear volume deformation of the interface under the linear and rotational shear paths is similar, which is mainly related to the shear length of the interface and has little relationship with the shear path; the reversible shear volume change rate is closely related to the stress ratio. Tianliang Wang et al. conducted an experimental study on the shear stress response, shear strength, and shear strength interface of the soil–structure interface under freezing conditions using an improved roughness algorithm and obtained the shear stress–displacement characteristics of the soil–structure interface, strain hardening at room temperature and strain softening at negative temperatures [51]. Miad Saberie et al. discussed the basic influencing factors of soil–structure interaction and introduced a research method based on the ability to combine fragmentation with improving the elastoplastic constitutive stimulation of cyclic cumulative shrinkage in particle interface modeling [52]. Considering the difference between the marine soil environment and the land-based soil, Kong Lingwei et al. [53], Yan Shuwang et al. [54] and Guo Jukun et al. [55] conducted shear tests on the interface between marine sand and marine soft clay and structures, respectively. The effects of initial undrained strength, degree of consolidation, and degree of disturbance on the interfacial shear characteristics were investigated. In addition, in response to the development strategy for the South China Sea, Yujie Li et al. [56] studied the effects of cementitious materials and surface roughness on the interfacial shear strength of the calcareous sand in the South China Sea dominated by coral debris.

At present, the weakening effect of soft marine soil has also been studied at home and abroad. Andersen [57] conducted a series of dynamic single shear and dynamic triaxial compression tests and tensile tests using undisturbed soil. The concept of cyclic shear strength was introduced. Bea [58] analyzed the influence of cyclic load loading rate and stress reversal on the weakening of soft soil foundations through experiments. Especially in the field of petroleum, due to the effects of deep-sea internal waves and temperature differences between the inside and outside, stress concentration and even buckling occur at the interface between the oil and gas pipeline and the soil, resulting in liquefaction or softening of the interface, resulting in pipeline instability. Hans Henning Stutz and Frank Wuttke proposed a low-plastic interface model for fine-grained and coarse-grained soils with the concept of intergranular strain, considering monotonic and cyclic interface phenomena for the interface between marine structures and soils [59]. Lin Cui [60] et al. investigated the stability of the foundation around the estuarine breakwater by means of a sub-model of the seabed. Oscillation and residual liquefaction phenomena were studied using poroelastic and poroelastic seafloor models, where loosely deposited soils are more prone to liquefaction under larger wave action.

Unlike the conventional interface, in natural gas hydrate production, the interface involves the coupling of multiple processes of phase transition, heat transfer, seepage, and deformation, resulting in the weakening of the interface. At the same time, the lack of

solid skeletons caused by mining sand also affects the mechanical behavior of the interface. However, the existing research on mechanical response and deformation mechanisms does not fully consider these factors. The research on the interface mechanical response mechanism under the condition of multi-process coupling with phase transition is the key to establishing the constitutive model of the interface between deep-sea soil and gas hydrate production wells.

(3) constitutive model

Over the last two decades, a multitude of models has been used to predict the behavior of soils under both monotonic and cyclic loading. The interaction between soil and structure has a significant impact on the interface model. The constitutive model of the interface is the stress–strain relationship of the interface. The first generation of interface models was elastic in nature and was followed by hyperbolic models. In the early days, the research on the interface mainly focused on the tangential stress–strain relationship. Later, the influence of the normal stress–strain was gradually paid attention to. The tangent, the normal stress–strain relationship, and the coupling relationship between the two were gradually studied in depth. At present, the elastic constitutive model for the interface is mainly nonlinear. Among them, the hyperbolic constitutive model proposed by Clough and Duncan [38] reveals the nonlinear relationship between the tangential stress and strain of the interface and is widely used to simulate the mechanical properties of the interface under normal stress and monotonic shear conditions. The model is simple, intuitive and easy to measure parameters, but there are still obvious defects. Peterson [45] and others further verified the applicability of their model and obtained a set of model parameters as a critical data source for analyzing the interaction between soil and structure. However, this model cannot reflect the phenomenon of interface softening and does not consider conditions such as cyclic shearing and tangential stress reversal, nor does it involve the coupling of tangential and normal deformations. In 1943, Ramberg and Osgood proposed a smooth model to describe the stress–strain skeleton curve and hysteresis curve of the material, referred to as the R–O model. In view of these defects, Desai [40] et al., based on the test results, considered the tangential stress reversal, interface hardening with cyclic cycles, normal stress, sand relative density, maximum shear displacement, and other influencing factors, and established a cyclic shear the interface modifies the R–O model under the action. Lu Tinghao [61] et al. established a simple coupled constitutive model for thin-layer interface elements considering shear volume deformation. With the deepening of the research on the interfacial shear properties, the elastic constitutive model cannot fully explain the interfacial shear properties. Based on the results of mesoscopic analysis, some scholars believe that the failure of the interface is rigid plasticity or ideal plasticity and establish related models [37,62,63]. However, the rigid–plastic and ideal elastic–plastic models are relatively simple constitutive models that cannot consider interface dilatancy, hardening, or softening properties Luan Maotian and Wu Yajun [64] proposed a nonlinear elastic–ideal plastic model for the interface between soil and structure and derived and established the stress–strain relationship and the elastoplastic coefficient matrix of the contact element. In the formula, r represents the degree to which the stress state reaches plasticity: when r = 0, it is an elastic state; when r = 1, it is a completely plastic state; when 0 < r < 1, it is a transition state from elastic to plastic.

$$[D_{ep}] = [D_e] - r\frac{[D_e]\left\{\frac{\partial f}{\partial \sigma}\right\}\left\{\frac{\partial f}{\partial \sigma}\right\}^T[D_e]}{\left\{\frac{\partial f}{\partial \sigma}\right\}^T[D_e]\left\{\frac{\partial f}{\partial \sigma}\right\}} \quad (1)$$

X.S.LI and Y. F.DAF ALIAS [65] have written on how the classical stress dilatancy theory in its exact form ignored the extra energy loss due to the static and kinematic constraints at particle contacts. It obstructs unified modeling of the behavior of cohesionless soils over a full range of densities and stress levels, considers shear swellability as a state-related quantity within the framework of critical-state geomechanics, combining the

internal state of the material with the basic concepts of critical-state geomechanics to solve the general expression and basic requirements of shear swell.

Daichao Sheng [66] et al. proposed a complete finite element treatment for unsaturated soil problems. For the first time, a new formulation of the general constitutive equation for unsaturated soils was presented. In the incremental stress–strain equation, the suction or pore water pressure was considered as a strain variable instead of a stress variable. In the paper by David W. Airey and Javad Ghorbani [67], the developed fully coupled dynamic finite element analysis and constitutive model for unsaturated soils was used for parametric studies, showing the ability to run up to 2500 cycles and simulate cyclic loading and simultaneous consolidation and drainage based on numerical analysis results. Yannis F. Dafalias [68] et al. established the SANICLAY model as a new simple anisotropic clay plasticity model, which is based on modifications of earlier models and associated flow rules, and can accurately simulate the undrained and drainage rate-independent behavior of normally consolidated sensitive clays and has satisfactory accuracy for overconsolidated clays. Javad Ghorbani [69] et al. developed a theoretical and numerical framework using a mortar-type contact algorithm for the elastoplastic interaction of unsaturated granular soils with rigid cylinders in static and dynamic analysis, and the present constitutive model provides the ability to simulate the effect of stress-induced anisotropy on the plastic response.

Sun Jizhu and Wang Yong [70] established an elastoplastic incremental constitutive relation, used tangential plastic work as the hardening parameter, described the interface friction coefficient as a hyperbolic function of plastic work, and completed the derivation of the incremental stress–displacement relationship, where $i, j = t, n$; $p, q = t, n$. H is the plastic hardening modulus, and M considers the change of the yield function with the development of plastic work or particle breakage, and explored the critical effect of particle breakage on the mechanical interface properties.

$$\begin{gathered} F = |\sigma_n \sin\alpha_k + \sigma_t \cos\alpha_k| + \mu(\sigma_n \cos\alpha_k + \sigma_t \sin\alpha_k) \\ Q = |\sigma_n \sin\alpha_k + \sigma_t \cos\alpha_k| \end{gathered} \tag{2}$$

$$\mathrm{d}\sigma_i = E_{ij}\left\{\mathrm{d}u_i - \frac{\frac{\partial F}{\partial \sigma_p} E_{pq}\mathrm{d}u_q}{\frac{\partial F_1}{\partial \sigma_p} E_{pq}\frac{\partial Q}{\partial \sigma_q} - H - M}\frac{\partial G}{\partial \sigma_j}\right\} \tag{3}$$

$$\mu = \frac{W^p}{a + bW^p} \tag{4}$$

At the same time, Luo Jia and Yao Yangping [71] proposed four basic stress–strain curve forms of low-confined, medium-confined, high-confined, and critical-confined interfaces based on extensive consideration of the typical stress–strain relationship of the interface. The shear dilatation equation is used to describe the coupling relationship between the interface shear strain and the volume change. The new dilatation equation is modified on the basis of the original Cambridge model and the de-dilation equation of the unified hardening model to describe the critical dilatancy characteristics of the interface.

$$\frac{\mathrm{d}\varepsilon_n^p}{\mathrm{d}\varepsilon_s^p} = M_f - \eta \qquad (original\ cambridge\ model) \tag{5}$$

$$\frac{\mathrm{d}\varepsilon_n^p}{\mathrm{d}\varepsilon_s^p} = M_{pt} - \eta \quad (Unified\ Hardening\ Dilation\ Equation) \tag{6}$$

On this basis, according to $|\xi - \eta| < |M_{pt} - \eta|$, where ξ is the parameter of the contact surface dilatation function reflecting the contact surface dilatation characteristics. When $\xi = M_f$, the proposed dilatation equation reflecting the properties of the contact surface degenerates into the original Cambridge model. When $\xi = M_{pt}$, it degenerates into the unified hardening dilation equation.

$$\frac{\mathrm{d}\varepsilon_n^p}{\mathrm{d}\varepsilon_s^p} = \xi - \eta \tag{7}$$

(*The dilatation equation reflecting the dilatancy characteristics of the contact surface*)

In the study of mechanical interface properties, many scholars have discovered the physical state evolution of the interface during the shearing process, and based on this, the concept of damage has been introduced into the establishment of the constitutive interface model to better simulate the interface shear mechanical properties. Based on the proposed concept of damaged state and the disturbed state concept, Desai [72,73] established an interface damage constitutive model. The incremental constitutive equations for the interface are given by the authors, which was verified by the results of cyclic tests at the interface between sand and concrete, where τ^a and σ_n^a are observed shear and normal stresses, respectively; ur and vr are the shear and normal relative displacements, respectively; $\mathbf{C}^i$ is the constitutive matrix for the RI response obtained from the plasticity theory with F; $\mathbf{C}^c$ is the constitutive matrix for the fully adjusted model; and D denotes increment $\tau_R = \tau^c - \tau^i$; and $\sigma_{nR} = \sigma_n^c - \sigma_n^i$.

$$\begin{Bmatrix} \mathrm{d}\tau^a \\ \mathrm{d}\sigma_n^a \end{Bmatrix} = (1-D)\mathbf{C}^i \begin{Bmatrix} \mathrm{d}u_r^i \\ \mathrm{d}v_r^i \end{Bmatrix} + D\mathbf{C}^c \begin{Bmatrix} \mathrm{d}u_r^c \\ \mathrm{d}v_r^c \end{Bmatrix} + \mathrm{d}D \begin{Bmatrix} \tau_R \\ \sigma_{nR} \end{Bmatrix} \tag{8}$$

Hu Liming and Pu Jialiu [74] also established a constitutive damage model to describe the monotonic mechanical properties of the interface between sand and rough structures. The damage evolution process is the gradual transformation process from the non-damage state to the critical state. Javad Ghorbani and David W. Airey [69] developed a constitutive model used to describe the anisotropy of the behavior of multiphase granular soils and the associated characteristics and established a computational framework for numerical simulations. The model is formulated based on the concept of effective stress in the unsaturated state, which ensures a smooth transition between the unsaturated and fully saturated states and is applicable to the soil state during hydrate reservoir extraction.

$$F = \frac{\tau^{i2}}{D_s} + \varepsilon_s^p \left[\tau^j - \mathrm{sign}\left(\tau^i\right) \cdot \sigma \tan \delta_0\right] = 0 \tag{9}$$

The contact surface in the damage-free state is described by the elastic–plastic constitutive relation. The following formula shows the yield function, where δ_0 is the friction angle, ε_s^p the plastic shear strain, D_s the shear elastic modulus, and the superscript i represents the non-damaged state.

An ideal plastic model describes the contact surface in the critical state, and its stress–strain relationship is shown in the following formula, where δ_0 is the residual friction angle, ε_v^c the volumetric strain in the critical state, ε_v^c the maximum volumetric strain of the soil, K is the volumetric strain parameter in the critical state, which is related to the roughness R and has nothing to do with the normal stress σ; D_r is the initial relative density of the soil; and σ_0 is a constant generally taken as 10 KPa. The superscript c indicates a critical state.

$$\begin{cases} \tau^e = \mathrm{sign}\left(\tau^i\right) \cdot \tan \delta_r \cdot \sigma \\ \varepsilon_v^c = \varepsilon_v^0 \left[1 - D_r - \exp\left(-K \frac{\sigma}{\sigma_0}\right)\right] \end{cases} \tag{10}$$

According to the damage state variable evolution law, it is assumed that the damage evolution process is only related to the plastic shear strain of the contact surface, and the damage state variable is $D = 1 - \exp\left(-a\left|\varepsilon_s^p\right|b\right)$. Combined with the basic principles of damage mechanics, according to the relationship between the stress–strain state variables, the elastic–plastic damage matrix is deduced. D_{sn} and D_{ns} can reflect the coupling effect of the normal and tangential directions of the contact surface. The model includes nine parameters: strength parameter δ_0, contact surface elasticity δ_r, shear stiffness D_s, elastic normal stiffness D_n, damage evolution parameters a, b, maximum body strain parameter of soil ε_v^0, and relative density. y D_r and soil critical state volume variable parameter K.

$$[D^{ep}] = \begin{bmatrix} D_{ss} & D_{sn} \\ D_{ns} & D_{nn} \end{bmatrix} \tag{11}$$

Pradhan and Desai [75] established a unified constitutive model considering the softening, hardening, and liquefaction properties of the interface. Zhang Ga [76–79] et al. proposed the interface elastic–plastic damage constitutive model based on the state evolution phenomenon in the shear test of the coarse-grained soil and the structure interface, taking the normalized form of the irreversible shear volume deformation as the damage factor; the two-dimensional static and dynamic characteristics of the contact surface between the coarse-grained soil and the structure are uniformly described, and the three-dimensional mathematical extension is carried out based on the test results. Using the mapping projection length as the internal variable, the plastic shear deformation modulus, and the internal variable were established; the change of the mapping point was used to reflect the turning point of the stress route. The new concepts of dividing the dilatation strain into reversible and irreversible dilatation strain and effective shear strain are introduced, and an incremental mathematical description of the elastic–plastic damage model of the interface between coarse-grained soil and structure is established.

$$\begin{aligned} \mathrm{d}\gamma &= \left(\tfrac{1}{G_\mathrm{e}} + \tfrac{1}{H_\mathrm{r}}\right)\mathrm{d}\tau - \tfrac{1}{H_\mathrm{rd}}\tfrac{|\tau|}{\sigma}\mathrm{d}\sigma \\ \mathrm{d}\varepsilon_\mathrm{v} &= \tfrac{\frac{1}{\mu}+n_\mathrm{a}+A_1}{H_\mathrm{r}}\mathrm{d}\tau + \left(\tfrac{C+C_\mathrm{e}}{\sigma} - \tfrac{\frac{1}{\mu}+n_\mathrm{a}+A_1}{H_\mathrm{rd}}\tfrac{|\tau|}{\sigma}\right)\mathrm{d}\sigma \end{aligned} \tag{12}$$

Sun Jizhu and Shi Geliang [80] established the interface plasticity model between sand and structure by introducing the damage factor into the elastic modulus based on the boundary interface theory. The model considers the effects of the initial relative density and normal stress of sand and can reflect the hysteresis and hardening characteristics of the interface tangential stress–strain under the action of cyclic shearing. By ignoring the coupling effect of the tangential and normal directions, the incremental stress–strain relationship on the contact surface is written as the following formula, where σ is the normal stress; τ is the shear stress; ε_n is the normal strain; and ε_s is the shear strain. Assuming that the damage is only related to the plastic shear strain, the damage parameter $\omega = 1 - \exp\left(-\mathrm{d}\varepsilon_\mathrm{s}''\right)$ is introduced, and the relative density of the critical state is fitted to complete the establishment of the two-dimensional boundary interface damage model.

$$\begin{Bmatrix} \mathrm{d}\tau \\ \mathrm{d}\sigma \end{Bmatrix} = \begin{bmatrix} G_\mathrm{s} & \\ & K_\mathrm{n} \end{bmatrix} \begin{Bmatrix} \mathrm{d}\varepsilon_\mathrm{s} \\ \mathrm{d}\varepsilon_\mathrm{n} \end{Bmatrix} \tag{13}$$

The deformation of the contact area includes two deformation mechanisms, continuous soil deformation and discontinuous dislocation in this area. The current research generally refers to the contact interface deformation without distinguishing between the two in the macroscopic view. It is assumed that the contact area strain has no gradient change. Most of the current constitutive models of the contact interface study the relationship between the deformation and stress of the contact interface. The currently used nonlinear elastic model, traditional elastic–plastic model, constitutive damage model, constitutive perturbation model, and state-dependent elastic–plastic constitutive model are only suitable for the monotonic loading mode and lack the description of unloading and reloading processes. Although nonlinear elastic models, ideal elastic–plastic models, and elastic–plastic constitutive models can reflect the basic characteristics of contact surfaces under cyclic loading conditions, the current advanced interface constitutive models mainly lack engineering applications for two-dimensional conditions [81].

In summary, the research results of the constitutive model of the interface between conventional soil and structure have been abundant, but the research on the static and dynamic laws of the interface between hydrate-bearing soil and mining well under the multi-process coupling is still insufficient. A constitutive model considering the evolution of mechanical interface properties under phase transition conditions has not been established to accurately describe the problem. At the same time, in order to analyze the influence of the hydrate extraction process on the physical and mechanical behavior of the sedimentary

layer, it is necessary to carry out a large number of physical and mechanical characteristics experiments and establish corresponding models for prediction. The establishment of constitutive models of hydrate sediments can be divided into three categories: nonlinear elastic constitutive models, elastic–plastic constitutive models, and constitutive models established by analogy to the damage theory of frozen soil. Different from other sediments, the stress–strain relationship and the dilatancy relationship of hydrate sediments are not only related to the effective stress state, temperature, stress and deformation history, particle composition, pore morphology, etc. Moreover, it is affected by factors such as hydrate saturation and hydrate occurrence form.

3. Interaction between Natural Gas Hydrate Production Well and Soil under Multi-Process Coupling

Wellbore integrity evaluation for natural gas hydrate production requires an accurate description of the interaction between the production well and the soil under the action of multi-process coupling. On the soil side, different from other oil and gas reservoirs, natural gas and water in hydrate reservoirs form hydrates, which form the reservoir skeleton together with soil mineral particles in the form of solids. Under the phase transition condition, the hydrate decomposes into gas and liquid and flows under the action of pressure difference, and the seepage characteristics of the reservoir change greatly due to the lack of framework. Therefore, the hydrate reservoir is a very special and enhanced fluid–structure interaction field [82]. Permeability of hydrate-bearing formation is affected by mineral particle size and gradation, porosity, hydrate saturation, and other factors [83]. The seepage of water and gas will affect the temperature field through thermal convection, and changes in the temperature field and pressure field will affect the decomposition and formation of hydrates [84]. Minagawa [85] studied different types of hydrate-containing sediments and found that their permeability depends on the pore size of fluid channels, and the presence of hydrates will reduce the absolute permeability of sediments. The results of core scouring experiments also show that the permeability of hydrate sediments decreases with the increase in hydrate saturation [86]. The core experiment study of the Nankai [87] continental slope in Japan shows that the permeability of sediments containing hydrate is positively correlated with the effective porosity. Delli [88] et al. conducted permeability test experiments under different saturations and proposed a mixed-weight model to describe the relationship between the permeability of hydrate-bearing soil layers and the storage state and saturation of hydrates. The relative permeability is predicted using the weighted combination of both the grain coating and the pore-filling model, where $k_{r\delta}^{pf}$ and $k_{r\delta}^{gc}$ are the relative permeabilities obtained from Kozeny grain coating and pore filling models, α and β the corresponding weighting parameters that are functions of underlying hydrate saturations.

$$k_{r\delta} = \alpha(S_h)k_{r\delta}^{pf} + \beta(S_h)k_{r\delta}^{gc} \tag{14}$$

Many scholars have researched the multi-field coupling model of temperature seepage deformation in hydrate-bearing formations. The earliest models for coupling fluid and thermal analysis were proposed by Goel [89] and Kurihara [90,91], respectively. However, they did not consider the effect of hydrate decomposition on soil stress–strain relationship and dilatancy relationship. To date, only a few coupled models have been used to simulate the gas hydrate production process [92]. Kimoto et al. [93] first tried to couple geomechanics and fluid heat to analyze the effect of hydrate decomposition on soil deformation and strength, but the model is extremely complex, with many parameters, and cannot analyze the strain-softening phenomenon caused by hydrate decomposition. Rutqvist [94] et al. worked with the TOUGH+HYDRATE program and used FLAC for semi-coupling calculation, realizing the combination of geotechnical mechanics and hydrate decomposition simulation. However, it is difficult to accurately simulate the stress release phenomenon caused by hydrate decomposition using this model, and this semi-coupling only considers the effects of heat and fluid on the mechanics of hydrate-bearing sediments but does not

consider the effects of the reverse process. Klar [95] et al. established a four-field multiphase coupled model of heat transfer seepage deformation-phase transformation to simulate the mechanical behavior of hydrate-bearing sediments during hydrate production. The model can reasonably simulate the stress-releasing phenomenon caused by hydrate decomposition. However, the strain-softening phenomenon is not considered. Kakumoto [96] developed a set of programs, Cotham, that can couple multiple fields and include the influence of multiphase gas, which is currently widely used in the basic experimental simulation research related to AIST gas hydrate, but there are few related papers published. In general, the current research on hydrated soils only superimposes the theoretically existing multiple processes (phase change heat transfer, gas–liquid seepage, etc.), and the research on the interaction between various mechanisms is not sufficient.

In addition to the soil side, the pressure field and temperature field in the wellbore during production are other boundary conditions for the evaluation and analysis of the wellbore integrity. The pressure field and temperature field in the wellbore during the production process are determined by the multiphase flow in the wellbore. In the process of hydrate production, the hydrates in the soil are decomposed into gas and water and, together with the hydrate solid particles enter the wellbore, forming a three-phase multi-component fluid (three-phase: gas, liquid, solid, multi-component; multi-component: methane, water, hydrate solid particles, geotechnical particles, etc.) in the wellbore. The temperature and pressure changes in the wellbore are not only affected by the gas production rate of the reservoir but also by the artificial lift method (such as an electric submersible pump or screw pump). For example, the separation efficiency of an electric submersible pump gas–liquid separation device is about 70%~80% [97,98]. The separated liquid passes through the electric submersible pump to cool the motor and then carries the motor to generate heat. This part of the heat will be transferred to the hydrate-containing low-temperature formation (the part below the mud line) step by step through the fluid, casing, cement, and formation interface in the subsequent wellbore flow, resulting in the decomposition of hydrate at the interface between the formation and the cementing cement, resulting in the generation of the micro annulus at the interface.

During the exploitation of natural gas hydrate deposits, the temperature of the decomposed natural gas gradually decreases during the flow of the decomposed natural gas along the wellbore to the wellhead. At this time, the dissolved water in the natural gas is separated out, forming a gas–water two-phase flow. Under suitable pressure and temperature conditions, secondary hydrate formation may occur [99] (Figure 4), plugging the wellbore and causing a series of problems: (1) flow assurance problem; (2) large pressure difference in the well before and after plugging; (3) hydrate formation releases heat to the wellbore wall. In the process of depressurization production, since the decomposition of hydrate is an endothermic reaction, additional energy needs to be added to the formation. It is a feasible method to use an intermittent injection of hot water to prevent the second generation of hydrate in the well. These factors all affect the temperature field and pressure field in the wellbore and thus affect the integrity of the production wellbore. In addition, the water production of hydrate gas wells is much larger than that of conventional natural gas wells (up to 100 times) [100], so hydrate gas wells require a larger wellbore and casing size to ensure economic commercial production. Meanwhile, for larger wellbores, undoubtedly, higher requirements are put forward for wellbore stability and wellbore integrity during drilling and production. At present, there are few studies on wellbore integrity in the process of natural gas hydrate extraction at home and abroad. Li Lingdong [101] et al. established a finite element model of the effect of drilling fluid temperature on the wellbore stability of gas hydrate formations. The simulation analysis shows that an increase in the temperature in the wellbore will lead to the expansion of the hydrate decomposition range, and at the same time, the formation strength will be reduced, and the mechanical properties will have deteriorated.

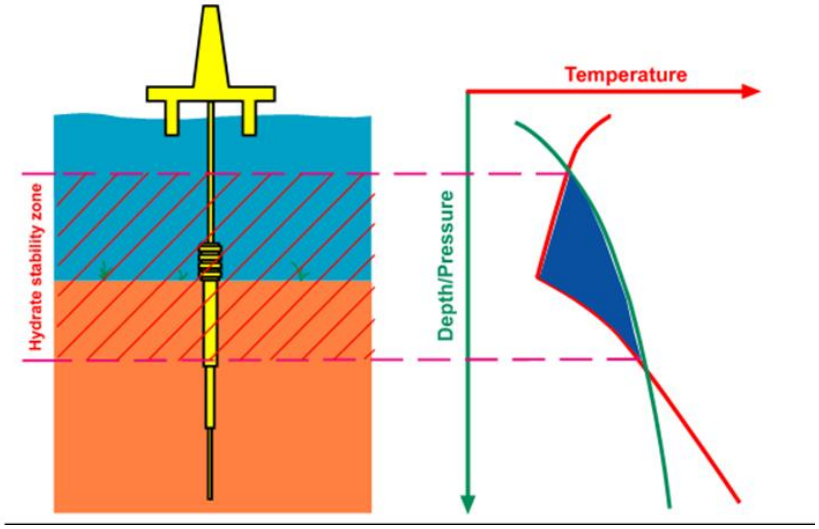

Figure 4. Temperature and pressure curve of natural gas hydrate production [This figure was modified with permission from ref. [99]. Copyright 2017, Deng, Z. et al.].

To sum up, the integrity assessment of natural gas hydrate production wellbore requires an accurate description of the interaction between the production well and the soil under the action of multi-process coupling. The interaction involves a system (hydrate-bearing soil–wellbore structure) and two boundary conditions (wellbore side, soil side). However, in the conventional wellbore integrity analysis, the special mechanical behavior of the interface between the soil and the wellbore and its weakening effect is not considered, resulting in problems in predicting the stress field around the wellbore. At the same time, in the process of gas hydrate extraction, the application of boundary conditions such as temperature field and pressure field on the wellbore side is determined by the multiphase flow in the wellbore; the complex multi-processes caused by hydrate decomposition coupling effect also needs to be considered in the evolution of the stress field on the soil side. The precise description of these factors affects the accuracy of wellbore integrity analysis for hydrate production and needs to be studied urgently.

4. Wellbore Integrity Assessment

Wellbore integrity is the key bottleneck restricting hydrate production. Wellbore integrity is the application of technical, operational, and organizational methods to reduce (and lower) the risk of uncontrolled escape of formation fluids throughout the life of a well. Natural gas hydrate is very sensitive to temperature and pressure, and changes in formation pressure and temperature around the wellbore during drilling will inevitably lead to the decomposition of hydrate in the formation. Hydrate-bearing formations are unconsolidated, weakly consolidated, or fractured formations. Once the hydrates that act as cementation or skeleton support are decomposed, the wellbore will collapse. The substantial subsidence of the formation will cause deformation or even buckling of the casing, causing relative slippage between the formation and the wellbore, resulting in a high-conductivity channel for gas and liquid leakage. The gas–water two-phase fluid generated by the decomposition increases the pore water content, reduces the effective stress, and weakens the inter-granular connection in the formation, causing the formation sand to block the wellbore, which will seriously damage the integrity of the wellbore's production [102–106].

A key step in wellbore integrity assessment is to quantitatively determine the stress state around the wellbore at different stages of the oil and gas well life cycle so as to provide an accurate judgment on how the integrity fails. If the analysis of the stress state around the wellbore is not accurate, unreasonable or even incorrect solutions will be given. Due to the complexity of downhole working conditions, it is still difficult to accurately determine

the stress state around the wellbore. In response to these problems, many scholars have carried out related research work. Yin Youquan [107] and others superimposed the casing loads solved by different stress condition formulas, and gave the elastic analytical solution of casing–surrounding rock combination under the action of non-uniform in situ stress, and obtained the finite element verification.

$$\begin{cases} \sigma_n = \sigma_n^A + \sigma_n^B = (s_1 + s_2)\cos\ 2\theta \\ \tau_n = \tau_n^A + \tau_n^B = s_3 \sin\ 2\theta \end{cases} \tag{15}$$

$$\begin{aligned} s_1 &= \frac{(1-v_s)(\sigma_H+\sigma_h)}{1+\frac{1}{1-m^2}\frac{1+v_c}{1+v_s}\frac{E_s}{E_c}(1-2v_c+m^2)} \\ s_2 &= -\frac{C_{22}+C_{12}}{C_{11}C_{22}-C_{12}C_{21}}\frac{2\left(1-v_s^2\right)}{1+v_c}\frac{E_c}{E_s}\left(1-m^2\right)^3(\sigma_H-\sigma_h) \\ s_3 &= \frac{C_{21}+C_{11}}{C_{11}C_{22}-C_{12}C_{21}}\frac{2\left(1-v_s^2\right)}{1+v_c}\frac{E_c}{E_s}\left(1-m^2\right)^3(\sigma_H-\sigma_h) \end{aligned} \tag{16}$$

Wan Xichao et al. [108] used the finite element method to analyze the casing cement sheath–surrounding rock combination mechanical analysis under the condition of non-uniform in situ stress and casing eccentricity; Li Jing [109] used the stress and displacement continuum method, combined with elastic mechanics and thermal stress theory to solve the theoretical solution of thermal stress of the casing–cement sheath–surrounding rock system.

Chu Wei [110] et al. carried out continuous internal pressure variation elastoplastic analysis of the casing–cement sheath–surrounding rock combination. A model for the plane strain problem of a thick-walled cylinder is established, assuming that the casing and surrounding rocks are elastic bodies and the cement sheath is an ideal elastic–plastic body. The yield condition satisfies the Mohr–Coulomb criterion. When the internal pressure exceeds a certain critical value, the cement sheath completely enters the plastic state, and there is no elastic zone.

$$\begin{cases} u_{so} = u_{cpi} \\ u_{cpo} = u_{cei} \\ u_{ceo} = u_{fi} \\ p_p = C\cot\varphi\left[\left(1+\frac{p_1}{C\cot\varphi}\right)\left(\frac{r_p}{r_1}\right)^{B-1}-1\right] \\ p_2 = \frac{1}{r_2^2(A+\sin\varphi)}\left[\left(Ar_2^2+r_p^2\sin\varphi\right)p_p-\left(r_2^2-r_p^2\right)C\cos\varphi\right] \end{cases} \tag{17}$$

Existing analysis methods for wellbore integrity are generally applicable to onshore production processes. For deep-sea gas hydrate exploitation, the reservoir is poorly cemented and buried in a shallow depth, which is very different from the wellbore integrity failure mode of on-road oil and gas exploitation. The study of wellbore integrity in the production process of natural gas hydrate is an important factor determining whether the natural gas hydrate can be successfully exploited. Scholars around the world have also conducted a lot of research in recent years. Manoochehr Salehabadi et al. established a numerical model for the development of gas hydrate-containing sediments to study the effect of gas hydrate decomposition on casing integrity due to rising wellbore temperature during deep-sea drilling [111]. Coupled flow and geomechanics play an important role in the analysis of producing gas hydrate reservoirs. The tightly coupled sequential approach proposed by J. Kimetal provides a rigorous two-way coupled model that captures the interrelationship between geomechanics and flow properties and processes, accurately describing system behavior that can be applied to hydrate behavior in geological media large-scale problems [112]. Ali Fereidounpour and Ali Vatanit designed and manufactured a set of experimental devices to study the behavior of hydrates in contact with drilling fluids with higher temperatures by studying the thermal stimulation mechanism of natural gas hydrate production and tested several muds containing different additives to study the key influencing factors of maintaining the integrity of the wellbore [113]. Kaibin

Qiu et al. evaluated the wellbore integrity of a methane hydrate production test well in the South China Sea trough by proposing a new workflow that can be applied to meet the heterogeneity and near-wellbore geometry of the entire oilfield formation. The results of the study are consistent with the 2013 Japan production test results. The model has the function of identifying wellbore integrity [98]. Saeed M. Golmohammadi and Ali Nakhaee developed a three-dimensional numerical model to simulate the hydrate dissociation behavior in porous reservoir media during drilling, using the model to deeply study the effect of wellbore pressure and temperature on dissociation pressure and temperature, dissociation front velocity and position, and gas production and the effect of the rate of gas release into the wellbore [114]. Tsubasa Sasaki et al. aim at the easy interference during the wellbore construction process in the weak form of natural gas hydrate exploitation, which leads to the loss of wellbore integrity and the occurrence of sand production, a simulation method of the wellbore construction process is proposed to evaluate the stress/ the area and magnitude of strain perturbations and the relative impact of each stage of construction on formation integrity [115]. Zhiqiang Liu et al. carried out a preliminary study on the geomechanical properties of gas hydrate-bearing sediments and wellbore integrity evaluation during the production process and established relevant models [15]. Shengyu Jiang et al. considered that the hydrate wellbore integrity degradation has obvious man–machine and complex system characteristics and established a layered control and closed-loop model for gas hydrate production wellbore systems. Wellbore integrity is related to executors' strategic preference and frequency of maintenance and supervision, as studied through game theory [116]. Chen Zhaoyang et al. combining the actual data of the second trial production in China, the simulation of hydrate depressurization production was carried out, and the gas/water production characteristics of the production well and the change characteristics of the temperature field, pressure field, and hydrate saturation field in the production area were analyzed, and then the permeability was analyzed. With the influence mechanism of rate, inter-well interference on pressure field, temperature field, and flow field change, the research results can be used for wellbore stability analysis [117]. Chang Yuanjiang et al. applied the natural gas hydrate wellbore–soil three-dimensional nonlinear coupling model established by combining fluid–solid coupling theory to a hydrate production well in the South China Sea to analyze wellbore stability factors. The subsidence of the layer and the upward uplift of the underlying stratum cause a large axial compressive stress in the wellbore in the reservoir section. The wellbore stability is controlled by the axial stress of the wellbore, and the maximum casing axial stress is located in the middle of the casing of the reservoir section, where the depressurization is produced [118]. Jiaxin Sun et al. used a numerical simulation method to study the wellbore stability based on the first exploratory well in the Shenhu area of the South China Sea. Through this model, it was concluded that gas hydrate with higher absolute permeability would dissipate more quickly from surrounding sediments the excess pore pressure, thereby contributing to wellbore stability [119].

For several hydrate test mining in the world, a great common challenge is the problem of sand production, which eventually leads to the end of the test mining in a short period, and the long-term stable mining cannot be realized (see Table 1).

Sand production usually refers to the phenomenon that during the production process of oil and gas wells, due to excessive production pressure difference and loose reservoir cementation, formation sand flows into the wellbore, blocking oil and gas passages, and causing oil and gas wells to stop production. Unlike the sand production problem in the development of conventional oil and gas reservoirs, there is a phase transition in the development of hydrate reservoirs, and its sand production and sand control face greater challenges. The sand production process is shown in Figure 5. Therefore, it is necessary to deeply analyze the control factors and control mechanisms that affect hydrate sand production. In general, the critical conditions for sand production of the formation depending on the reservoir strength parameters. For hydrate reservoirs, the reservoir parameters, in turn, depend on the hydrate decomposition process. In the process of

hydrate decomposition, the distribution state of hydrate, the arrangement of framework particles, and the mechanical parameters of the reservoir all change with time [120].

Table 1. Hydrate mining method and sand control technology.

Project	Reservoir Properties	Mining Method	Whether Sand Controlled and Effects
Messo Yaha, former Soviet Union (1967)	Depth 700~800 m; thickness 84 m; sandstone	Reduce pressure, inject chemicals	Perforation completion; poorly unconsolidated sand production of gas hydrate reservoir
Mackenzie, Canada (2002, 2007–2008)	Depth 800~1100 m; thickness 110 m; sandstone	2002, heat injection 2007, reduce pressure + heat injection 2008, reduce pressure	Mechanical sand control; sand production perforation completion; not sand controlled; ESP damage caused by sand production mechanical sand control; add sand prevention meshwork to pump inlet; sand production
Alaska North Slope (2008, 2012)	Thickness 40~130 m; saturation 75%; sandstone	Reduce pressure, Carbon dioxide replacement	Perforated sand screen for sand control; sand production
Japan's sea of love (2013)	Water depth 1000 m; burial depth 300 m; sandstone	Reduce pressure	Open-hole gravel sand screen for sand control; sand production caused the failure of the ESP work and was forced to terminate
Japan's South China Sea Trough (2017)	Thickness 50 m	Reduce pressure	Geoform sand control system, the pre-expand of Geoform sand control system and geoform sand control system which expands after going down well (active)
Shenhu, South China South (2017)	Water depth 1266 m; burial depth 203~277 m; silty mud reservoir	Formation fluid extraction	the sand control of undiagenetic ultrafine reservoir; effective sand control
Liwan, South China Sea (2017)	Water depth 1310 m; buried depth 117~196 m; non-diagenetic reservoir	Solid-state fluidized mining	without sand control, the sand was separated from gas, water and hydrate inside the lifting pipeline
Shenhu, South China South (2020)	Water depth 1255 m; burial depth 203~277 m; silty shale reservoir	Formation fluid extraction	An innovative combination of bypass pipe technology and pre-packed screen technology, a new type of bypass pre-packed screen was developed; sand control is effective

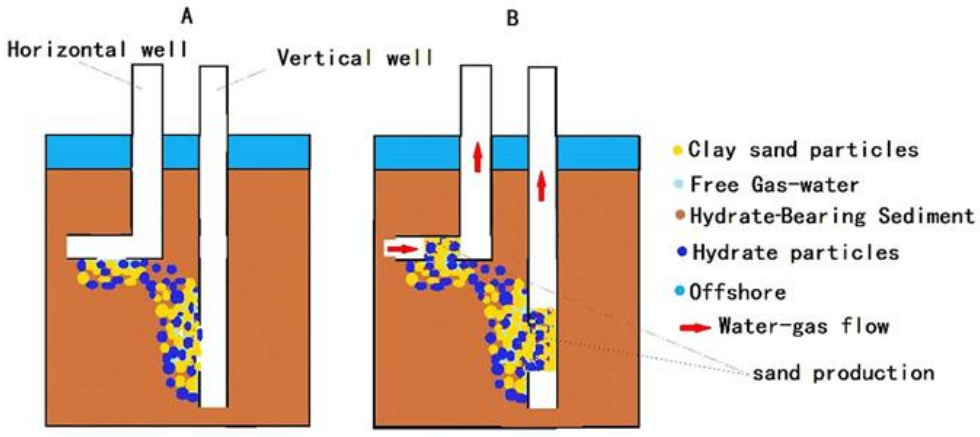

Figure 5. Schematic diagram of (**A**) hydrate-bearing sediment (exploitation in the horizontal and vertical wells) and (**B**) sand production during hydrate exploitation [This figure was modified with permission from ref. [121]. Copyright 2021, American Institute of Physics].

Many scholars have conducted research on the sand production process of hydrate mining. Oyama et al. [122] found that sand production occurred during the depressurization process of hydrate instability, and the water flow rate was the main factor affecting sand production. Jung [123] et al. studied the effect of fine particles on hydrate mining and found that the migration and plugging of fine silt particles are mainly affected by relative geometric constraints and clearly pointed out that even with low fine silt content, its impact on hydration mining cannot be ignored. Based on the data of the first trial mining in Japan in 2013, Murphy et al. [124] built a hydrate sand production test device, combined with the critical model of geotechnical mechanics, and mainly considered the sand production under two critical conditions of loose sand and compact sand. Sand production was found to be related to the porosity and confining pressure of the sediment. Uchida [125–128] et al.

established a theoretical model of heat transfer-seepage–deformation sand production in hydrate formations, revealing that the uneven stress distribution of low-saturation hydrate reservoirs leads to shear deformation of high-hydrate-saturation reservoirs. Ning [129] used the TOUGH+HYDRATE model to simulate the depressurization production process of hydrate. The results show that the increase in bottom hole pressure difference will lead to the increase in seabed subsidence and the corresponding increase in sand production, but it does not affect the short-term normal test production. For long-term test production operations, it is necessary to balance the relationship between productivity, reservoir stability, and sand production. A large number of scholars have explored the mechanism of hydrate sand production, the damage to hydrate reservoirs caused by sand production, and sand control methods through numerical simulation and experimental research. Tianbo Yu observed the movement and blockage of fine sand by developing a sand production simulator with a visualization function and concluded that fluid flow rate and initial hydrate saturation are important factors affecting sand production under different working conditions [130]. C. Yan et al. believe that although the existing test mining has taken effective sand control measures, its effectiveness needs to be further verified because the mining scale and time are far from reaching the commercial scale. Effective sand control measures should ensure both wellbore stability and product stability. It is necessary to establish a large-scale sand-producing reservoir instability early warning mechanism for hydrate reservoirs and to improve the sand treatment capacity of the platform [131]. Huixing Zhu et al. combined the characteristic data of natural gas production and storage published in two test productions in Japan, considering sand production and sand control devices and using a numerical simulation method to evaluate the gas production and water production of production wells. The production strategies used also fail to meet commercial extraction standards and require the introduction of new technologies [132]. Shanshan Zhou et al. tested the median particle size ratio to be 6.5 and conducted a sand migration test. The appearance of sand bridge structure in the pore space of the sample is an important phenomenon in the process of hydrate decomposition, which is beneficial to gas production and sand control [133]. Yongmao Hao et al. constructed a numerical model through the sand–gas–water multiphase flow process in the reservoir and concluded that due to the high concentration of migrating sand, the settlement of sand is mainly concentrated near the wellbore. The reduction in reservoir porosity and permeability caused by sand settlement has a significant impact on production. The effect of sand production on reservoir fluid mobility shows that fluid flow near the wellbore is inhibited, while fluid flow performance is improved farther away from the wellbore [134]. Jiping Ding et al., by introducing the plastic-softening-stage, established a thermal-fluid–solid coupling mathematical model of sand production based on the destruction of reservoir skeleton and hydrate transformation, which truly simulated the sand production process under wellhead pressure reduction and analyzed the sand production mechanism and change rule from the perspective of rock mechanics. Sand production first appears at the position where the principal horizontal stress is the smallest. The whole sand production process can be divided into three stages: initial sand production, large-scale sand production, and stable sand production, which continuously erodes the wellhead [135]. Yurong Jin et al. used the clay-silt sediment utilization test method in the Shenhu area of the northern South China Sea to simulate the seepage, stress–strain field, and sand production characteristics of the sediment around the wellbore after hydrate decomposition to observe the sandstone failure mode as a follow-up theoretical formula providing the basis for model building [136]. Jingsheng Lu et al. developed a set of sand production and sand control test systems that can be used to analyze the sand production and sand control in the hydrate mining process, which has guiding significance for the actual hydrate reservoir sand production and sand control [121]. Jinze Song et al. studied the effects of hydrate saturation, effective confining pressure, sand content, hydrate distribution, and multi-physics on sand production during hydrate mining and numerically simulated the current sand production problems. Discuss experimental research methods and point out that machine learning and optimization methods can be used for theoretical

research on sand production and sand control [137]. Xiangyu Fang et al. researched clay silty hydrate reservoirs through experimental methods and found that with the increase in clay content, the sand production of natural gas hydrate first increases and then decreases. When the clay content is 20%, the sand production reaches the maximum value, and the sand production is the largest before the hydrate decomposition, and the sand production decreases significantly after the decomposition [138]. Yiqun Zhang et al. conducted experiments with sand screens of different mesh numbers and found that vertical wells with gravel packing combined with sand control screens, radial wells combined with gravel packing and sand control screens had less sand production, and radial well gas production rate and recovery rate of composite sand control method are better [139]. Chuanliang Yan et al. established a thermal-fluid–solid coupling chemical model for hydrate production by carbon dioxide replacement and concluded that although the existence of carbon dioxide hydrate inhibits the decomposition of methane hydrate, it improves the formation strength and reduces the risk of sand production. The larger the scope of carbon dioxide hydrate formation, the lower the risk of sand production [140]. Ya-Ting Xu et al. used a new experimental device to study the sand production behavior of quartz sands with different particle sizes in methane hydrate reservoirs and studied the relationship between particle size and reservoir damage through decompression dissociation hydrate experiments [141]. Pengwei Zhang et al. established a model that considers the detachment, migration, and settlement of fine particles in pore space to characterize fine particle migration and plugging of multiphase flow in gas hydrate reservoirs, and applied the model to in situ gas hydration in the South China Sea Trough testing, calibration and long-term yield forecasting [142]. Haiyan Zhu et al. performed triaxial compression tests by synthesizing methane hydrate sand to capture the mechanical response, developed a discrete element method (DEM) model to examine the mechanical response and verified the model reliability through Duncan–Chang model embedding [143]. Xiao-Yan Li et al. conducted decompression and dissociation experiments on sand control screens with different mesh numbers in a new hydrate simulator and at the same time, analyzed the gas–liquid sand production behavior and found that the increase and decrease in the screen mesh number sand production and medium density. However, it also increases the resistance, which leads to a decrease in gas production. For economical sand control screen selection, it should not be too large or too small (Figure 6) [144]. Jiping Ding et al. conducted tests on four different types of sand control elements in the South China Sea gas hydrate storage and discussed sand control and plugging mechanism from a microscopic perspective in combination with factors such as pressure, temperature, permeability, sand production, and reservoir skeleton structure (see Figure 6) [145].

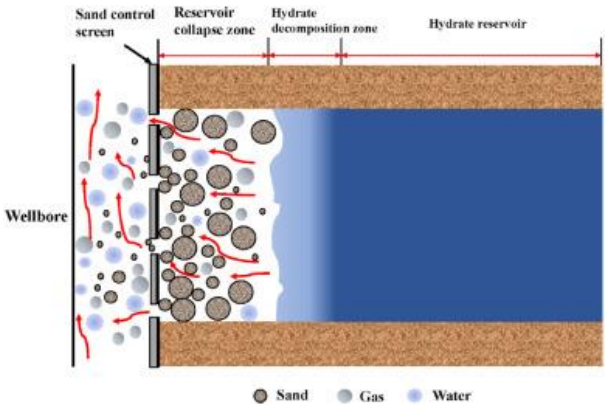

Figure 6. Schematic diagram of sand control in the exploitation of a vertical well in the NGH reservoir [This figure was modified with permission from ref. [144]. Copyright 2022, Elsevier].

Bin Gong et al. considered the effect of mining scale on the stability of the submarine slope and sand production near the wellbore by numerical simulation method.

Additionally, the deformation response of the ocean slope is analyzed by the lower thermal-fluid–mechanical coupling model, and it is concluded that the sand production always starts from the upper and lower sections of the methane hydrate sediments around the wellbore [146]. Xiangyu Fang et al. experimentally analyzed the effects of hydrate saturation and overburden stress on the sand production behavior of sand-bearing, hydrate-bearing sediments before, during, and after hydrate dissociation by depressurization. It is concluded that the amount of sand produced before the decomposition of hydrate is small, the amount of sand produced during decomposition increases significantly, and the amount of sand produced increases with the increase in hydrate saturation. When the overburden force increases, the sand production first increases and then decreases. After the stress reaches the critical value, the friction between particles may become the main controlling factor [147]. To sum up, many scholars in the world have conducted a lot of research on the problem of sand production in the process of hydrate mining through the combination of theory and experiment. The establishment of an innovative experimental device provides a favorable tool for the sand production mechanism and prevention of sand production in the hydrate mining process (see Figure 7).

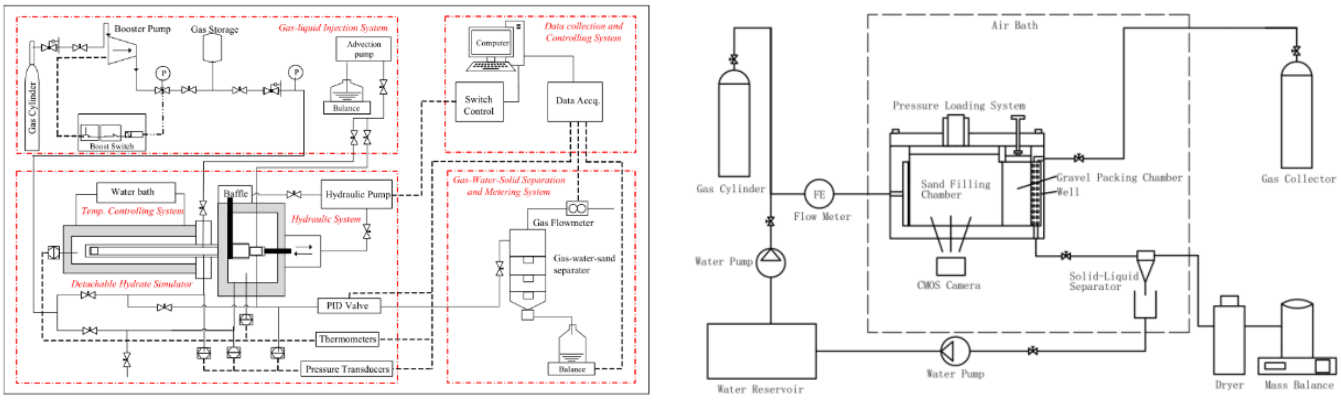

Figure 7. Hydrate sand production simulator [This figure was modified with permission from ref. [138,145]. Copyright 2021, 2022, Elsevier].

In addition to the problem of sand production, after the decomposition of natural gas hydrates, the mechanical properties of the sediments change signhaodificantly, and the elastic modulus decreases, which causes the stress state of the formation to change after the hydrate extraction, leads to large deformation of the formation after long-term extraction, affects the stability of the production well, causes stratum subsidence, and even causes a wide range of submarine landslides and stratum subsidence, which damages the wellhead and the submarine manifold and leads to the failure of the test production project. Therefore, wellhead stability is crucial in the process of natural gas hydrate exploitation. Establishing a model for formation subsidence and wellhead stability guides the safe development of natural gas hydrate. Currently, most natural gas hydrate development technologies follow traditional oil and gas development technologies, and conventional deep-water oil and gas development has involved much work on wellhead stability. During the installation process of conventional deep-water wellheads, there are wellhead subsidence accidents due to low stratum strength and poor diagenesis, resulting in insufficient stratum bearing capacity. After the riser installation is completed, the complex load transmitted to the wellhead due to the comprehensive action of floating drilling platform drift, selection of soil–pile contact model, tension setting on the riser top, and environmental load causes the wellhead to undergo large bending deformation and tilting. Due to the complexity of the formation parameters in the deep sea and shallow layers, the complexity of parameter design in the process of jetting and running the surface conduit leads to the failure of the conduit to be run in place and unable to provide sufficient bearing capacity, burying hidden dangers for the long-term stability of the wellhead.

Yanbin Wang et al. established two different soil–pile contact interface models to calculate the lateral displacement and vertical bearing capacity. In order to ensure the stability of the wellhead, it is recommended to use different soil–pile contact models to calculate the conductor bearing capacity and use the minimum value as the conductor design basis. The vertical bearing capacity of the conductor string is mainly composed of friction resistance force on side wall and supporting force on end of conductor. If ignoring the mutual influence between them, the limit vertical bearing capacity Q_{umax} of the conductor string can be represented as such, where U_i is soil thickness of i layer, m; l_i is the circumference of the conductor, m; q_{sui} is the soil ultimate frictional resistance stress on per unit area of the side wall, kPa; A_p is the conductor end area, m^2; and q_{pu} is ultimate resistance stress on per unit area of end, kPa in Figure 8 [148].

$$Q_{umax} = Q_{\mathrm{famx}} + Q_{pamx} = \sum_{i=0}^{I} U_i \times l_i \times q_{\mathrm{sui}} + A_p \times q_{pu} \quad (18)$$

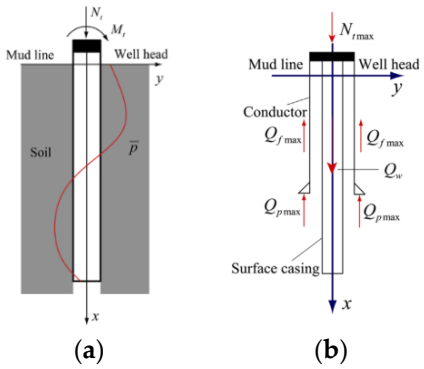

(**a**) (**b**)

Figure 8. (**a**) Pile and soil interaction analysis model. (**b**) Vertical bearing capacity model [This figure was modified with permission from ref. [148]. Copyright 2014, Elsevier].

Jiayi Li et al. proposed a local stress–strain method based on a semi-decoupled model to predict wellhead fatigue life more accurately. In the semi-decoupled model, the subsea wellhead was modeled by the combination of a beam with round section and a non-linear spring as shown in Figure 9. H is the height of the beam, EI is the flexural stiffness of the beam, K is the stiffness of the non-linear spring, and Hst is the height of the spring from the top of the beam [149].

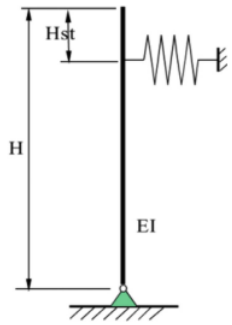

Figure 9. Equivalent model of subsea wellhead. [This figure was modified with permission from ref. [149]. Copyright 2020, Elsevier].

Wei Yan et al. established an analysis model for the stability of underwater wellhead in deep-water drilling by using the method of numerical simulation of pile element and nonlinear spring element in ANSYS [150]. Iwona Adamiec-Wójcik and Stanisław Wojciech studied the space model of the riser dynamics developed by the proposed method and its application through experimental and numerical simulation results. It is concluded that the

movement of the upper end of the riser compensates for the horizontal movement of the base and stabilizes the force in the connection of the riser to the wellhead [151]. Wenlong Li et al. evaluated the stability of the wellhead using composite casing by establishing a mechanical model. The composite casing structure has better stability than the previous conventional jet conductors, and the composite casing composed of larger conductors has better stability and lower horizontal displacement and vertical load. Once the horizontal displacement profile is obtained, the bending moment, deflection angle, and shearing force profiles can be calculated as follows (see Figure 10) [152]:

$$\begin{cases} \theta_i = -\frac{y_{i+1}-y_{i-1}}{2h} \\ M_i = -\frac{(EI)_i(y_{i+1}-2y_i+y_{i-1})}{h^2} \\ Q_i = -\frac{(EI)_{i+1}y_{i+2}-\left[2(EI)_{i+1}-N_ih^2\right]y_{i+1}+(EI)_{i-1}y_{i-2}}{2h^3} \\ \frac{\left[(EI)_{i+1}-(EI)_{i-1}\right]y_i+\left[2(EI)_{i-1}-N_ih^2\right]y_{i-1}}{2h^3} \end{cases} . \quad (19)$$

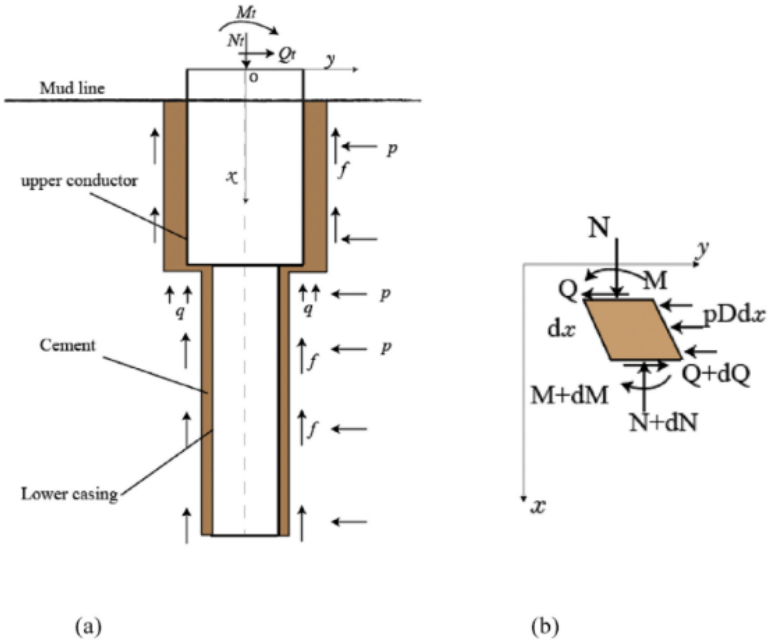

Figure 10. Mechanical analysis diagram of composite casing–cement structure [This figure was modified with permission from ref. [152]. Copyright 2020, Elsevier].

Yuqiang Xu et al. carried out stress and strain analysis on the subsea wellhead system, and at the same time, based on dimensionless processing and sensitivity analysis, the factors that have a greater impact on the wellhead stability were obtained [153]. Su Kanhua et al. analyzed the overall force of the subsea wellhead system for deep-water drilling, established the wellhead mechanical stability analysis method, and determined the influencing factors affecting the stability of the subsea wellhead [154]. De and Yan Wei use the pipe element and nonlinear spring element in ANSYS to simulate the force and deformation process of the pipe–soil connection, analyze the lateral displacement of the subsea wellhead, the rotation angle of the wellhead and the bending moment of the pipe body, and complete the stability analysis of the subsea wellhead [155]. Based on the Ansys finite element analysis software, Zhang Jianping established and applied the strength check of the deep-water drilling surface conduit and the underwater wellhead stability analysis model. The equivalent stress of the first surface conduit of the underwater wellhead is checked, respectively, when the wellhead is not tilted and tilted at different angles, and the maximum displacement of the platform under the basis of safe operation is obtained [156]. Zhou Rongxin et al. established the mechanical analysis model of the

subsea wellhead system and the deflection differential equation of the subsea wellhead to analyze the influence of different top tensions on the stability of the subsea wellhead and concluded that the axial load top tension is the only controllable factor affecting the wellhead stability. The calculation method based on the minimum top tension is used in the calculation of deep-water drilling, and setting the tension ratio of 1.0 to 1.5 times is beneficial to improve the stability of the subsea wellhead system. In the differential equation of wellhead deflection, EI is the bending stiffness of the wellhead, N m^2; y is the deflection at a certain position x along its length, m; N is the axial load, N; p is the soil reaction per unit length force, N [157].

$$EI\frac{d^4y}{dx^4} + N\frac{d^2y}{dx^2} - p = 0 \quad (20)$$

Jin Yang et al. analyzed the factors affecting wellhead stability, such as conduit parameters, soil properties, engineering parameters, and environmental loads, to provide a reference for wellhead stability research [158]. Xiaodong Wu et al. analyzed the force of the subsea wellhead before and after the installation of the deep-water drilling riser and BOP, and concluded that the vertical load, drilling fluid density and bending moment are not significantly affected by the top tension, but the lateral load, top tension and the mud discharge height of the pipe have great influence. Yi Wu et al. used the SACS analysis software to analyze the strength and stability of a single riser based on the displacement conditions obtained from the overall analysis of the light-duty fixed simple platform used in the offshore oilfield [159]. Qingchao Li et al. evaluated the effects of hydrate dissociation and wellhead stability through numerical simulation, and concluded that the continuous dissociation of hydrates in homogeneous and isotropic formations would cause a nonlinear increase in the vertical displacement of the wellhead. The displacement of the wellhead will increase with the subsidence of the overlying strata, and the shallower and thicker hydrate reservoir will aggravate the impact of hydrate decomposition on the wellhead stability (see Figure 11) [160].

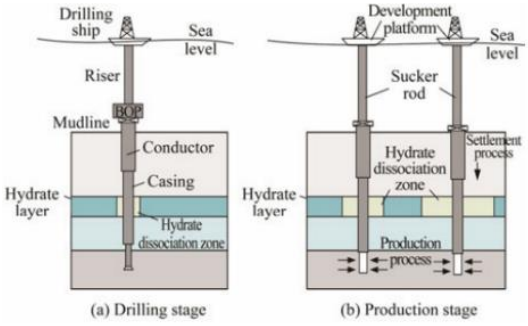

Figure 11. Sketch of wellhead instability caused by hydrate dissociation during the OGD process in deep water [This figure was modified with permission from ref. [160]. Copyright 2018, Springer].

Lele Yang et al. analyzed the soil deformation and stability around the wellhead in the process of gas hydrate extraction. When the dip angle of the seabed soil layer is constant, the decomposition area and deformation amount of the soil body increases continuously. When the hydrate decomposition is within the critical value, the deformation of the soil around the wellhead is limited; after the critical value is exceeded, the surrounding soil will undergo shear damage, and the degree of hydrate decomposition plays the most critical role in the wellhead stability [161]. Li Lilin et al. analyzed the wellhead instability factors in the process of natural gas hydrate production by establishing an analysis model of seabed strata subsidence and wellhead stability in the process of trial production of hydrate in non-diagenetic strata. The finite element strength reduction method was used to simulate and study the effect of hydrate decomposition on formation subsidence and wellhead stability. It is concluded that the negative friction resistance around the pipe string after hydrate decomposition is mainly distributed in the upward 1/3 area from the bottom of the

surface conduit, and the larger the hydrate decomposition radius and the higher the hydrate saturation, the greater the negative friction resistance. At the same time, the reliability of the numerical simulation is verified by the self-developed gas hydrate mining wellhead simulation device [162]. Due to the special geological structure of hydrate reservoirs and the instability of deep-water and shallow formations, the application of special wellhead systems can effectively solve the wellhead stability and maintain efficient development of hydrate reservoirs. Kanhua Su et al. designed a conduit carrying capacity enhancement device through which conductors are connected during drilling and then sprayed to a specified depth. The large diameter of the device increases the contact area of the string with the soft soil, thus increasing the conductor axial load carrying capacity. In addition, the unit shares the moment of the riser, thereby increasing the lateral load-carrying capacity of the conductors (see Figure 12) [163,164]. Kan Changbin et al. designed a new duct assembly structure to improve the vertical and lateral bearing capacity of the duct and anchor the barrel-shaped foundation to the seabed mudline to increase the frictional contact area to maintain the vertical bearing capacity. It has a righting effect when it is subjected to bending moments and has a load sharing effect when it is subjected to complex loads. l_1 is the depth of penetration of the bucket foundation, m; l_j is the thickness of the soil layer j, m; U_{jn} and U_{jw} are the perimeters of the inner wall and outer wall of the bucket foundation in soil layer j, respectively, m; $q_{sun,j}$ and $q_{suw,j}$ are the ultimate pipe side resistances per unit area on the inner wall and outer wall of the bucket foundation in soil layer j, respectively, kN/m^2; A_t and A_b are, respectively, the top and the bottom ring areas of the bucket foundation, m^2; and q_{put} and q_{pub} are, respectively, the top and the bottom ultimate resistance per unit area, kN/m^2 (see Figure 13) [165].

$$Q_{\mathrm{umax},1} = N_{bo} + N_{bi} + N'_{\mathrm{bv}} + N_{bv} = \sum_{j=0}^{l_1} l_j \left(U_{jn} q_{sun,j} + U_{jw} q_{suw,j} \right) + A_t q_{put} + A_b q_{pub} \quad (21)$$

The water blowout preventer technology places the blowout preventer above the water surface and below the deck position, and the subsea wellhead is connected back to the drilling platform through a riser. Compared with the underwater blowout preventer, the water blowout preventer uses a smaller riser, and the cost of its own maintenance and supporting facilities is lower, which reduces the performance requirements of the drilling platform. When the water blowout preventer system is used for development, the running depth of the conduit is small, so the lateral load–displacement and bending moment are relatively small, and the overall wellhead stability is higher. It is suitable for complex environments, and the use cost is lower. It has been well used in Mexico and Brazil [166,167]. Suction pile foundations are often used as pile foundations for mooring systems, subsea production systems, and self-installing platforms during the development of offshore oil and gas fields [168]. The catheter is greatly shortened and integrated into the suction anchor to form a catheter suction anchor system, and the system is used to realize the penetration installation technology of the suction anchor to realize the construction of the surface layer. In order to solve the impact of the use of heavy-duty blowout preventers in deep polar water on the wellhead stability and to deal with emergencies such as drilling drift, the suction anchor surface well construction technology was first applied in the Norwegian Sea and the large cross-sectional area of the suction anchor conduit and the absorbed soil quality improved the overall wellhead bearing capacity and bending resistance (see Figure 14) [169]. The suction anchor surface well construction technology greatly shortens the well structure while providing sufficient bearing capacity and high installation efficiency, which can provide a stable operating environment for the drilling stage. It has good applicability for the test production of marine hydrate, and also has great application potential in the drilling and production of deep-water shallow resources in the future, which can effectively solve the problems of wellhead subsidence and instability. A prediction model of catheter suction anchor penetration resistance was derived. Q_{a} is the penetration resistance of the catheter suction anchor, kN; Q_{sc} is the side wall resistance of the catheter suction anchor,

kN; Q_{tc} is the resistance at the end of the suction anchor of the catheter, kN; d_o is the outer diameter of the outer cylinder of the catheter suction anchor, m; d_i is the inner diameter of the outer cylinder of the catheter suction anchor, m; d is the outer diameter of the inner cylinder of the catheter suction anchor, m; and l is the penetration depth of the inner tube of the catheter suction anchor, m [170].

$$\begin{gathered} Q_a = Q_{sc} + Q_{tc} \\ Q_{sc} = z\pi d_o \alpha_o S u_v + \pi(z d_i + L d)\alpha_i S u_v \\ Q_{tc} = \tfrac{1}{4}\pi\left(d_o^2 - d_i^2\right)\left(N_c S u_i + \gamma z\right) + \varepsilon U l (f + f_\sigma)\cos\alpha \end{gathered} \tag{22}$$

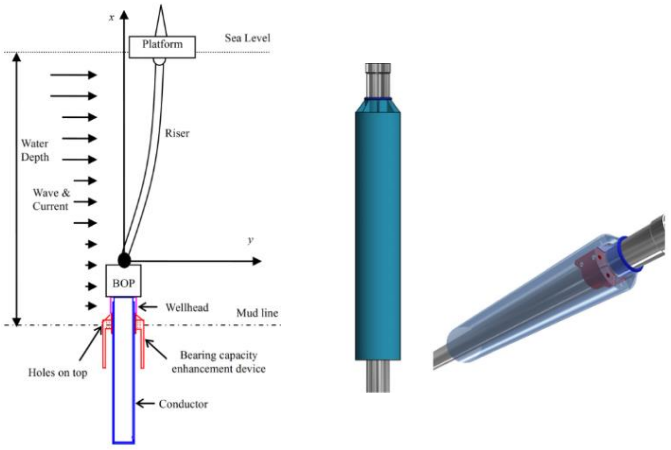

Figure 12. Conduit-bearing capacity strengthening device [This figure was modified with permission from ref. [164]. Copyright 2018, ASME].

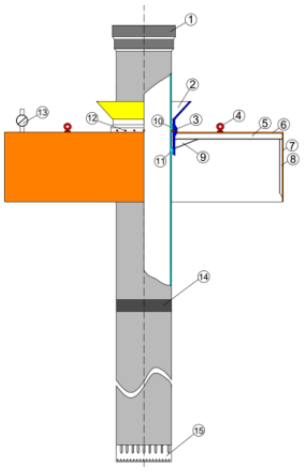

Figure 13. Conduit combination structure [This figure was modified with permission from ref. [165]. Copyright 2018, Elsevier].

Hydrate reservoirs in the Shenhu area of the South China Sea occur in fine-grained sediments such as argillaceous silt in shallow strata between tens of meters and 300 m below the seafloor mud surface. The subsea soft clay and argillaceous silt, whose overburden is mostly non-diagenetic, are considered to be the hydrate reservoirs with the largest reserves and the most difficult development. In 2017, China completed the first test production in the Shenhu area of the South China Sea, which confirmed the feasibility of development. The first test production time was relatively short, and the decomposition range of the gas hydrate reservoir was relatively small, so there was no problem with the subsidence of the submarine strata [171–175]. In 2020, China completed the second trial mining, and the

scale of the second trial mining was 5.57 times larger than the first. In order to deal with the problem of subsidence of the seabed strata, self-developed suction anchors are innovatively used. The surface well construction technology applied to the suction anchor ensures the stability of the wellhead in shallow soft formations. At the same time, the vertical and horizontal bearing capacity of the wellhead is provided for the deflection of the horizontal well. It provides a more extensive selection space for increasing the height of the kick-off point and reducing the kick-off requirements [6].

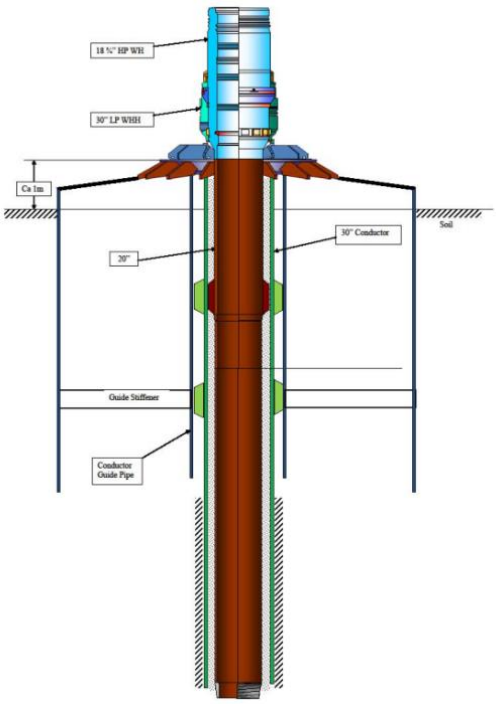

Figure 14. Surface well construction technology of suction anchor [This figure was modified with permission from ref. [169]. Copyright 2011, SPE].

To sum up, there are many wellbore integrity analysis studies for onshore oil and gas production. Deep-sea gas hydrate mining has poor reservoir cementation and shallow burial depth, which is quite different from the failure mode of wellbore integrity in onshore oil and gas production. Conventional oil and gas extraction reservoirs are deep, and generally, there is no problem with reservoir subsidence and collapse. However, deep-water hydrate reservoirs are located in shallow layers, and the skeleton of the reservoir is unconsolidated or weakly consolidated, which is likely to cause large subsidence and then collapse during the mining process, posing challenges to the safety of mining. At the same time, the problem of sand production and blockage in the hydrate mining process is the bottleneck problem that restricts large-scale commercial mining. Compared with conventional oil and gas sand production, the particle size of hydrate reservoirs is smaller, and the sand production process is accompanied by complex multi-process coupling of phase transition-heat transfer–seepage-deformation. Therefore, the problem of hydrate sand production is more complicated, and its sand production mechanism, shape, law, and main controlling factors have not been clarified, and further systematic and in-depth analysis is required.

5. Wellbore Integrity Evaluation System by the Interface Parameters for Hydrate Production

According to the structure type of deep-sea hydrate mining wells, the multi-process action characteristics such as variable temperature and pressure, material transport such as quicksand, and hydrate phase transition on the deep-sea soil–mining well interface

are mainly considered. The fabric evolution, such as the interfacial phase transition and the formation of macropores, is proved, and the correlation mechanism between the fabric evolution and the interface weakening characteristics is revealed. On this basis, a production well integrity analysis method considering the interface weakening is proposed.

The specific contents include:

(1) Research and development of test equipment and testing technology for deep-water hydrate extraction wells

   (i) Temperature–pressure precise dual-control interface shear test system: the modification of the direct shearing instrument for soil containing hydrate can carry out the monotonic and cyclic shear tests of the interface. On this basis, the interface temperature and pore pressure real-time control and measurement modules are further developed to realize the interface shear test under the condition of precise dual control of temperature and pressure. Develop a structure acquisition and measurement module for hydrates in the interface, and develop a real-time high-precision measurement system for the interface strain field combined with digital image correlation technology (DIC).

   (ii) Wellbore response physics test platform in the process of hydrate production: Based on the existing large-scale 3D physical model test equipment for hydrate production, develop a real-time measurement module for the temperature and deformation of the wellbore and its interface with soil, and integrate the research and development of depressurization water inflow units, sand production collect monitoring units and permeability measurement units to form a test module for hydrate mining and sand production.

(2) Revealing the coupling mechanism of interface weakening properties and fabric evolution under the condition of hydrate decomposition.

Absorb the research results of the deep-sea hydrate-bearing soil in Topic 1, and decompose the multi-process coupling characteristics experienced by the hydrate-bearing soil and the interface of the mining well. Consider the conditions of variable temperature and pressure, phase transformation, and sand production, respectively. Study the coupling mechanism of interface weakening characteristics and fabric evolution, and then comprehensively analyze the complete mechanism, including:

   (i) The influence of temperature and pore pressure changes on interface mechanical properties: changing normal boundary conditions, shear stress levels, and soil physical and mechanical parameters, etc. The interface direct shear test was carried out under the condition of no phase transformation, and the structural changes such as the stress–displacement response and porosity of the interface are observed. Based on the idea of combining macro and micro, the correlation mechanism between the weakening characteristics of the interface and the fabric evolution is analyzed, and the influence of temperature and pore pressure changes on the mechanical properties of the interface is revealed.

   (ii) Coupling mechanism of interface weakening properties and fabric evolution under phase transition conditions: change normal boundary conditions, shear stress levels, and soil physical and mechanical parameters, simulate hydrate phase transition, conduct interface direct shear tests, and interface the stress-displacement response, porosity change, and phase transition of the interface are observed, and the response of the missing solid skeleton and the output (gas, liquid) fluid involved in the decomposition process of the phase transition is measured. Based on the idea of combining macro and microscopic features, the correlation mechanism between interface weakening properties and fabric evolution, especially phase transition is analyzed, and the coupling mechanism between interface weakening properties and fabric evolution under phase transition conditions is revealed.

(iii) The influence of sand production on the interface weakening characteristics: simulate different sand production forms (pore liquefaction type, earthworm-like cave type, etc.). By changing the normal boundary conditions, shear stress levels and other factors, the direct shear test of the interface between the hydrate-containing soil and the structure was carried out, and the stress–displacement response and porosity of the interface after the sand mining were observed. Based on the idea of combining macro and micro, the correlation mechanism between interface weakening characteristics and fabric evolution is analyzed, and the influence law of sand production on interface weakening characteristics is revealed.

(iv) Coupling mathematical model of interface weakening characteristics and fabric evolution: comprehensively analyze the coupling characteristics of interface weakening characteristics and fabric evolution under the conditions of variable temperature and pressure, phase transition, and sand production, and obtain the interface weakening under multi-factor coupling mechanism, study the mathematical description of the mechanism, and establish a coupled-variable mathematical model of interface weakening characteristics and fabric evolution.

(3) Explore the failure mode of production wells considering interface weakening.

In view of the multi-process coupling characteristics of variable temperature and pressure, material transport such as quicksand and hydrate phase transition involved in hydrate mining, several typical hydrate mining methods are considered. Based on the coupling mechanism of interface weakening characteristics and fabric evolution, future research should focus on the complex interaction of wellbore–soil structure and failure modes of production wells, including:

(i) Interaction analysis of deep-sea soil and hydrate production wells: establishing multiphase flow control equations in the wellbore and calculating the evolution law of the temperature field and pressure field in the well during the production process; through multi-process coupled numerical simulation, the deep-sea soil phase transition, heat transfer, seepage, and deformation processes under the disturbance of the temperature field and pressure field in the well are studied, and the stress evolution around the well is obtained.

(ii) Exploration of the failure mode of wellbore integrity: based on the results of the above interaction analysis, combined with the response test simulation of the hydrate mining wellbore, the weakening process of the interface between the deep-sea soil and the mining well is studied; the failure modes of wellbore integrity, such as reservoir subsidence and collapse, sand production blockage, etc., are revealed under different mining techniques and working conditions.

(4) A wellbore integrity analysis method for hydrate production considering the interface weakening effect is proposed.

Compared with conventional oil and gas production, the particularity of the failure mode of wellbore integrity in hydrate production is mainly reflected in two aspects: sand production and collapse. By describing the interface weakening effect, the interaction between the hydrated soil and the wellbore can be reflected. Based on the understanding of the failure mode of the wellbore, an evaluation method for the integrity of the wellbore is proposed, which mainly includes the following two methods:

(i) Hydration prediction method of sand production in hydrate mining: summarize and analyze the sand production mechanism, sand production form, and plugging law under different hydrate production techniques and working conditions, as well as the main controlling factors of sand production in deep-sea hydrate production; sand production prediction model based on onshore oil and gas production, establish a deep-water hydrate mining sand production model with interface weakening effect under multi-process coupling conditions,

predict whether sand production, sand production amount and sand production form during the mining process and verify the effectiveness of the method by comparing with the model test.

(ii) Reservoir settlement prediction model and collapse evaluation method for hydrate extraction: summarize the main controlling factors and influence laws of reservoir settlement during hydrate extraction, and establish a deep-water hydrate extraction reservoir settlement prediction model. The interaction characteristics between the production well and the soil are analyzed, the mathematical description method of the relationship between the interface weakening and the failure mode is studied, and the evaluation criteria for reservoir collapse considering the interface weakening characteristics are proposed. Compared with the numerical simulation and model test results, the validity of the settlement prediction model and the collapse evaluation method is verified.

6. Conclusions

The biggest difference between hydrate extraction and conventional oil and gas extraction is that hydrates undergo a phase transition in the extraction process. During this phase transition process, the hydrate itself, which is a part of the reservoir skeleton, will decompose, resulting in the absence of the deep-sea soil solid skeleton and a decrease in soil strength. The decrease in soil strength, coupled with the fine particles and poor cementation of the hydrated soil itself, will cause serious sand production problems, resulting in a further lack of deep-sea soil solid skeleton and a serious weakening of the deep-sea soil–hydrate mining well interface. Natural gas hydrate reservoirs are prone to decomposition at shallow depths and are susceptible to natural and anthropogenic influences on the temperature and pressure of the subsea water during extraction. The cyclic response needs to be taken into consideration because the structures are subjected to wave loads during the extraction process, which can easily change the hydrate layer from a relatively stable state to an unstable state and lead to submarine soil liquefaction or submarine landslide. The unstable nature of hydrate reservoirs and the influence of cyclic response needs to be taken into consideration. In order to avoid wellhead destabilization due to geological changes in the soil during hydrate extraction. Meanwhile, hydrate decomposition is an endothermic process accompanied by the formation of gas and liquid fluids. Therefore, the phase transition process also involves changes in the interface temperature and pore pressure, which have an impact on the interface strength. For example, the generated gas and liquid fluids will increase the pore pressure, reduce the effective stress of the soil, and then cause damage to the interface. Phase transformation, sand production, temperature, and pore pressure changes are not involved in the traditional interface mechanical properties research. Therefore, the correlation mechanism between the weakening characteristics of the interface between deep-sea soil water and hydrate production wells and the phase transition is the primary key scientific problem to be solved in hydrate production.

Traditional wellbore integrity analysis generally does not consider interface mechanical properties and weakening effects, resulting in inaccurate calculation of wellbore stress and thus affecting the reliability of wellbore integrity assessment. In hydrate production, the interface weakening caused by changes in a phase transition, sand production, temperature, and pore pressure is closely related to the failure of wellbore integrity. At the same time, the hydrate reservoir is shallow in burial depth and poor in cementation, and the multi-process coupling of phase transition-heat transfer–deformation-seepage is involved in the production engineering, so the failure mode of wellbore integrity is very different from that of conventional oil and gas production: the problem of hydrate production produces sand blockage is very prominent, which increases the risk of settlement and collapse. Therefore, physical simulation tests and multi-process coupled numerical simulation methods are used to reveal the interaction characteristics of deep-sea soil and gas hydrate production wells and the failure mode of hydrate production wellbore integrity. Through the characterization of the interface weakening effect, the interaction between the hydrate-containing soil and

the production wellbore is reflected, and the influence of the interface weakening on the failure mode of the production well is explored. Furthermore, a wellbore integrity analysis method for hydrate production considering the interface weakening effect is proposed, which is the core key technical problem to be solved in hydrate production.

Deep-sea natural gas hydrate mining wells, through the research and development of deep-sea hydrate mining well test equipment and testing technology, focus on the phenomenon, law and mechanism of the interface weakening between deep-sea soil and hydrate mining wells. It focuses on achieving breakthroughs in three aspects: the weakening of the interface between deep-sea soil and hydrate mining wells, the failure of mining wells, and the analysis methods of wellbore integrity:

(1) Revealing the phase transition characteristics and weakening coupling laws of the interface between deep-sea soil and hydrate extraction wells and establishing a mathematical model of interface weakening characteristics considering the phase transition conditions;
(2) Revealing the multi-process interaction between deep-sea soil and hydrate mining wells, and exploring the failure mode of hydrate mining wells under mining disturbances;
(3) Establishing and proposing a wellbore integrity analysis method considering the interface weakening effect and form natural gas hydrate sand production prediction method and reservoir subsidence prediction model and collapse evaluation method.

Finally, it is hoped that the wellbore integrity analysis will be improved from "simple working conditions and simplified models" to "full life cycle complex working conditions, deep-sea soil and mining well collaborative working system model."

Author Contributions: Supervision, M.Z., M.D., R.Y., J.Z., Y.L. and S.G.; writing—original draft, M.Z., R.Y. and M.D.; writing—review and editing, M.D., Y.L. and S.G. All authors have read and agreedto the published version of the manuscript.

Funding: This research received no external funding.

Institutional Review Board Statement: Not applicable.

Informed Consent Statement: Not applicable.

Data Availability Statement: Not applicable.

Conflicts of Interest: The authors declare no conflict of interest.

References

1. Wei, N.; Bai, R.; Zhou, S.; Luo, Y.; Zhao, J.; Zhang, Y.; Xue, J. China's Deepwater Gas Hydrate Development Strategies under the Goal of Carbon Peak. *Nat. Gas Ind.* **2022**, *42*, 156–165.
2. Li, N.; Wang, J.; Liu, R.; Tang, X. Multi-scenario Conception on the Development of Natural Gas Industry under the Goal of Carbon Neutrality. *Nat. Gas Ind.* **2021**, *41*, 183–192.
3. Lee, S.Y.; Holder, G.D. Methane Hydrates Potential as a Future Energy Source. *Fuel Process. Technol.* **2001**, *71*, 181–186. [CrossRef]
4. Boswell, R.; Collett, T.S. Current Perspectives on Gas Hydrate Resources. *Energy Environ. Sci.* **2011**, *4*, 1206–1215. [CrossRef]
5. Luo, M.; Wang, H.; Yang, S.; Chen, D. Research Advancement of Natural Gas Hydrate in South China Sea. *Bull. Miner. Petrol. Geochem.* **2013**, *32*, 56–79.
6. Ye, J.; Qin, X.; Xie, W.; Lu, H.; Ma, B.; Qiu, H.; Liang, J.; Lu, J.; Kuang, Z.; Lu, C.; et al. Main Progress of the Second Gas Hydrate Trial Production in the South China Sea. *Geol. China* **2020**, *47*, 557–568.
7. Sahu, C.; Kumar, R.; Sangwai, J.S. A comprehensive review on well completion operations and artificial lift techniques for methane gas production from natural gas hydrate reservoirs. *Energy Fuels* **2021**, *35*, 11740–11760. [CrossRef]
8. Wei, H.; Yan, R.; Wei, C.; Wu, E.; Chen, P.; Tian, H. Summary of Researches for Phase-equilibrium of Natural Gas Hydrates in Bearing Sediments. *Rock Soil Mech.* **2011**, *32*, 9.
9. Fitzgerald, G.C.; Castaldi, M.J.; Schicks, J.M. Methane Hydrate Formation and Thermal Based Dissociation Behavior in Silica Glass Bead Porous Media. *Ind. Eng. Chem. Res.* **2014**, *53*, 6840–6854. [CrossRef]
10. Khlebnikov, V.N.; Antonov, S.V.; Mishin, A.S.; Bakulin, D.A.; Khamidullina, I.V.; Liang, M.; Vinokurov, V.A.; Gushchin, P.A. A New Method for the Replacement of CH_4 with CO_2 in Natural Gas Hydrate Production. *Nat. Gas Ind. B* **2016**, *3*, 445–451. [CrossRef]

11. Konno, Y.; Jin, Y.; Shinjou, K.; Nagao, J. Experimental Evaluation of the Gas Recovery Factor of Methane Hydrate in Sandy Sediment. *RSC Adv.* **2014**, *4*, 51666–51675. [CrossRef]
12. Ota, M.; Morohashi, K.; Abe, Y.; Watanabe, M.; Smith, R.L., Jr.; Inomata, H. Replacement of CH_4 in the Hydrate by Use of Liquid CO_2. *Energy Convers. Manag.* **2005**, *46*, 1680–1691. [CrossRef]
13. Pooladi-Darvish, M.; Hong, H. *Effect of Conductive and Convective Heat Flow on Gas Production from Natural Hydrates by Depressurization*; Springer: New York, NY, USA, 2004.
14. Uchida, S.; Klar, A.; Yamamoto, K. Sand Production Model in Gas Hydrate-bearing Sediments. *Int. J. Rock Mech. Min. Sci.* **2016**, *86*, 303–316. [CrossRef]
15. Liu, Z.; Lu, Y.; Cheng, J.; Han, Q.; Hu, Z.; Wang, L. Geomechanics involved in gas hydrate recovery. *Chin. J. Chem. Eng.* **2019**, *27*, 2099–2106. [CrossRef]
16. Zhang, J. New Advances in Basic Theories of Sand Dynamics. *Chin. J. Geotech. Eng.* **2012**, *34*, 50.
17. Li, G. The Six Disadvantages of the Rock Altar. *Miner. Explor.* **2006**, *3*, 20–22.
18. Feng, D.; Zhang, J. Influence of Initial Static Shear Stress on Cycle Mechanical Behavior of Interface between Structure and Gravelly Soil. *Rock Soil Mech.* **2012**, *33*, 7.
19. Feng, D.; Zhang, J. Monotonic and Cyclic Behaviors of Coarse-grained Soil-structure Interface Using Large-scale Simple Shear Device. *Chin. J. Geotech. Eng.* **2012**, *34*, 8.
20. Potyondy, J.G. Skin Friction between Various Soils and Construction Materials. *Géotechnique* **1961**, *11*, 339–353. [CrossRef]
21. Uesugi, M.; Kishida, H. Frictional Resistance at Yield between Dry Sand and Mild Steel-ScienceDirect. *Soils Found.* **1986**, *26*, 139–149. [CrossRef]
22. Desai, C.; Drumm, E.; Zaman, M. Cyclic Testing and Modeling of Interfaces. *J. Geotech. Eng.* **1985**, *111*, 793–815. [CrossRef]
23. Fakharian, K.; Evgin, E. Cyclic Simple-shear Behavior of Sand-steel Interfaces under Constant Normal Stiffness Condition. *J. Geotech. Geoenviron. Eng.* **1997**, *123*, 1096–1105. [CrossRef]
24. Gao, J.; Yu, H.; Zhao, W. Characteristics Study of Interface Between Soil and Concrete by Using Large Size Since Shear Apparatus and Numerical Analysis. *China Civ. Eng. J.* **2000**, *33*, 5.
25. Wang, J.; Zhou, Y.; Tang, X.; Huang, S. Development and Application of Large Size Direct Shear Test Apparatus with Visual and Digital Collection Functions for Reinforced soil. *Rock Soil Mech.* **2017**, *38*, 1533–1540.
26. Zhang, G.; Zhang, J. Development and Application of Cyclic Shear Apparatus for Soil-structure Interface. *Chin. J. Geotech. Eng.* **2003**, *25*, 149–153.
27. Xu, H.; Dai, S. Research Progress of Pile-soil Interface Shear Test Apparatus Under Temperature Effect and Manufacture of New Apparatus. *Bull. Sci. Technol.* **2019**, *35*, 139–142.
28. AbdelSalam, S.S.; Suleiman, M.T.; Sritharan, S. Enhanced Load-Transfer Analysis for Friction Piles Using a Modified Borehole Shear Test. *Geotech. Test. J.* **2012**, *35*, 879–889. [CrossRef]
29. Vogelsang, J.; Huber, G.; Triantafyllidis, T. A Large-Scale Soil-Structure Interface Testing Device. *Geotech. Test. J.* **2013**, *36*, 20120213. [CrossRef]
30. Eid, H.T. Undrained Interface Shear Strength of Fine-Grained Soils for Near-Shore Marine Pipelines. *Geotech. Test. J.* **2019**, *43*, 20180188. [CrossRef]
31. Liang, Y.; Xia, R.; Liu, Z.; Ma, C.; Zhang, H.; Sun, Z. Experimental Investigation into Cyclic Shear Behaviors in the Interface Between Steel and Crushed Mudstone Particles. *Transp. Res. Rec. J. Transp. Res. Board* **2021**, *2676*, 499–509. [CrossRef]
32. Xu, C.; Liao, X.; Ye, G.; Li, Z. Researches on Frictional Properties of HDPE Geomembrane Using Tilt Table Device. *Chin. J. Geotech. Eng.* **2006**, *28*, 989–993.
33. Cho, K.; Cho, J.R.; Chin, W.J.; Kim, B.S. Bond-slip Model for Coarse Sand Coated Interface between FRP and Concrete from Optimization Technique. *Comput. Struct.* **2006**, *84*, 439–449. [CrossRef]
34. Uesugi, M.; Kishida, H. Influential Factors of Friction between Steel and Dry Sands. *Soils Found.* **1986**, *26*, 33–46. [CrossRef]
35. Tsubakihara, Y.; Kishida, H.; Nishiyama, T. Friction between Cohesive Soils and Steel. *J. Jpn. Soc. Soil Mech. Found. Eng.* **1993**, *33*, 145–156. [CrossRef]
36. Yoshimi, Y.; Kishida, T. A Ring Torsion Apparatus for Evaluating Friction Between Soil and Metal Surfaces. *Geotechnol. Test. J.* **1981**, *4*, 8. [CrossRef]
37. Yin, Z.; Xu, G. Numerical Simulation of the Deformation in the Interface between Soil and Structural Material. *Chin. J. Geotechnol. Eng.* **1994**, *16*, 14–22.
38. Clough, G.W.; Duncan, J.M. Finite Element Analyses of Retaining Wall Behavior. *ASCE Soil Mech. Found. Div. J.* **1971**, *97*, 1657–1673. [CrossRef]
39. Bathe, K.-J.; Chaudhary, A. A Solution Method for Planar and Axisymmetric Contact Problems. *Int. J. Numer. Methods Eng.* **1985**, *21*, 65–88. [CrossRef]
40. Desai, C. Some Aspects of Constitutive Models for Geologic Media. In Proceedings of the Third International Conference on Numerical Methods in Geomechanics, Aachen, Germany, 2–6 April 1979.
41. Zeghal, M. In Soil Structure Interaction Analysis: Modelling the Interface, Engineering in Medicine & Biology. In Proceedings of the Conference & the Fall Meeting of the Biomedical Engineering Society Embs/Bmes, Second Joint, Houston, TX, USA, 23–26 October 2002.

42. Tsubakihara, Y.; Kishida, H. Frictional Behaviour between Normally Consolidated Clay and Steel by Two Direct Shear Type Apparatuses. *J. Jpn. Soc. Soil Mech. Found. Eng.* **1993**, *33*, 1–13. [CrossRef]
43. Zhang, G.; Zhang, J. Monotonic and Cyclic Constitutive Law of Interface Between Structure and Coarse Grained Soil. *Chin. J. Geotech. Eng.* **2005**, *27*, 515–520.
44. Hou, W. *Research on Monotonic and Cyclic Behavior and Constitutive Model of Three-Dimensional Soil-Structure Interface*; Tsinghua University: Beijing, China, 2008.
45. Peterson, M.; Kulhawy, F.; Nucci, L.; Wasil, B. *Stress-Deformation Behavior of Soil-Concrete Interfaces*; Contract Report B-49; Niagara Mohawk Power Corporation: Syracuse, NY, USA, 1976.
46. Boulon, M. Basic Features of Soil Structure Interface Behaviour. *Comput. Geotech.* **1989**, *7*, 115–131. [CrossRef]
47. Hryciw, R.D.; Irsyam, M. Behavior of Sand Particles around Rigid Ribbed Inclusions during Shear. *Soils Found.* **2008**, *33*, 1–13. [CrossRef]
48. Fakharian, K.; Evgin, E. An Automated Apparatus for Three-Dimensional Monotonic and Cyclic Testing of Interfaces. *Geotechnol. Test. J.* **1996**, *19*, 22–31.
49. Gomez, J.E.; Filz, G.M.; Ebeling, R.M. *Development of an Improved Numerical Model for Concrete-to-Soil Interfaces in Soil-Structure Interaction Analyses*; Technical Report ITL-99-1; Defense Technical Information Center: Fairfax, VA, USA, 1999.
50. Zhang, G.; Zhang, J. Reversible and irreversible dilatancy of soil-structure interface. *Rock Soil Mech.* **2005**, *5*, 699–704.
51. Wang, T.-L.; Wang, H.-H.; Hu, T.-F.; Song, H.-F. Experimental Study on the Mechanical Properties of Soil-structure Interface under Frozen Conditions Using an Improved Roughness Algorithm. *Cold Reg. Sci. Technol.* **2019**, *158*, 62–68. [CrossRef]
52. Saberi, M.; Annan, C.-D.; Konrad, J.-M. On the Mechanics and Modeling of Interfaces between Granular Soils and Structural Materials. *Arch. Civ. Mech. Eng.* **2018**, *18*, 1562–1579. [CrossRef]
53. Kong, L.; Xiong, C.; Guo, A.; Yang, A. Effects of Shear Rate on Strength Properties and Pile-soil Interface of Marine Soft Clay. *Chin. J. Geotech. Eng.* **2017**, *39* (Suppl. S2), 13–16.
54. Yan, P.; Lin, P.; Jia, Z.; Lang, R. Large-scale Direct Shear Tests on Shear Strength of Interface Between Marine Soil and Steel Piles. *Chin. J. Geotech. Eng.* **2018**, *40*, 495–501.
55. Guo, J.; Kou, H.; Xu, H.; Lei, S. Experimental Study on Shear Behaviors of Interface Between Pile and Marine Clay. *J. Yangtze River Sci. Res. Inst.* **2019**, *36*, 104–108, 117.
56. Li, Y.; Guo, Z.; Wang, L.; Li, Y.; Liu, Z. Shear Resistance of MICP Cementing Material at the Interface between Calcareous Sand and Steel. *Mater. Lett.* **2020**, *274*, 128009. [CrossRef]
57. Andersen, K.H.; Pool, J.H.; Brown, S.F.; Rosebrand, W.F. Cyclic and Static Laboratory Tests on Drammen clay. *J. Geotech. Eng. Div.* **1980**, *106*, 499–529. [CrossRef]
58. Bea, R.G. Pile capacity for axial cyclic loading. *Int. J. Rock Mech. Min. Sci. Geomech. Abstr.* **1992**, *29*, 34–50.
59. Stutz, H.H.; Wuttke, F. Hypoplasticmodeling of Soil-structure Interfaces in Offshore Applications. *J. Zhejiang Univ. Sci. A* **2018**, *19*, 624–637. [CrossRef]
60. Cui, L.; Jeng, D.S. Seabed liquefaction around breakwater heads at a river mouth: An integrated 3D model. *Ocean. Eng.* **2021**, *242*, 110036. [CrossRef]
61. Lu, T.; Bao, F. A Coupled Constitutive Model for Interface Thin layer Element. *J. Hydraul. Eng.* **2000**, *2*, 5.
62. Gens, A.; Carol, I.; Alonso, E.E. A constitutive model for rock joints formulation and numerical implementation. *Comput. Geotech.* **1990**, *9*, 3–20. [CrossRef]
63. Gens, A.; Carol, I.; Alonso, E.E. An interface element formulation for the analysis of soil-reinforcement interaction. *Comput. Geotech.* **1989**, *7*, 133–151. [CrossRef]
64. Luan, M.; Wu, Y. A Nonlinear Elasto-perfectly Plastic Model of Interface Element for Soil-structure Interaction and Its Applications. *Rock Soil Mech.* **2004**, *25*, 7.
65. Vatsala, A. Discussion: Dilatancy for cohesionless soils. *Géotechnique* **2001**, *51*, 729–730. [CrossRef]
66. Sheng, D.; Sloan, S.W.; Gens, A.; Smith, D.W. Finite element formulation and algorithms for unsaturated soils. Part I: Theory. *Int. J. Numer. Anal. Methods Geomech.* **2003**, *27*, 745–765. [CrossRef]
67. Airey, D.W.; Ghorbani, J. Analysis of unsaturated soil columns with application to bulk cargo liquefaction in ships. *Comput. Geotech.* **2021**, *140*, 104402. [CrossRef]
68. Dafalias, Y.F.; Manzari, M.T.; Papadimitriou, A.G. SANICLAY: Simple anisotropic clay plasticity model. *Int. J. Numer. Anal. Methods Geomech.* **2006**, *30*, 1231–1257. [CrossRef]
69. Ghorbani, J.; Nazem, M.; Kodikara, J.; Wriggers, P. Finite element solution for static and dynamic interactions of cylindrical rigid objects and unsaturated granular soils. *Comput. Methods Appl. Mech. Eng.* **2021**, *384*, 113974. [CrossRef]
70. Sun, J.; Wang, Y. Constitutive Model of Calcareous Sand Structure Interface. *Chin. Q. Mech.* **2006**, *27*, 5.
71. Luo, J.; Yao, Y. Dilatancy Behavior of Soil-structure Interfaces and Its Simulation. *Ind. Constr.* **2006**, *36*, 4.
72. Desai, C.S.; Ma, Y. Modeling of Joints and Interfaces Using the Disturbed State Concept. *Int. J. Numer. Anal. Methods Geomech.* **1992**, *16*, 623–653. [CrossRef]
73. Desai, C.S.; Pradhan, S.K.; Cohen, D. Cyclic Testing and Constitutive Modeling of Saturated Sand–concrete Interfaces Using the Disturbed State Concept. *Int. J. Geomech.* **2005**, *5*, 286–294. [CrossRef]
74. Hu, L.; Pu, J. Application the Damage Model to Soil Interface in Finite Element. *China Civ. Eng. J.* **2002**, *35*, 5.

75. Pradhan, S.K.; Desai, C.S. DSC Model for Soil and Interface including Liquefaction and Prediction of Centrifuge Test. *J. Geotech. Geoenviron. Eng.* **2006**, *132*, 214–222. [CrossRef]
76. Zhang, G.; Zhang, J. Unified Modeling of Soil-structure Interface and Its Test Confirmation. *Chin. J. Geotech. Eng.* **2005**, *27*, 1175–1179.
77. Zhang, G.; Zhang, J.M. Unified Modeling of Monotonic and Cyclic Behavior of Interface Between Structure and Gravelly Soil. *Soils Found.* **2011**, *48*, 231–245. [CrossRef]
78. Zhang, G. *A Study on the Static and Dynamic Characteristics and Elastic-Plastic Damage Theory of the Interface between Coarse-Grained Soil and Structure*; Tsinghua University: Beijing, China, 2002.
79. Zhang, G.; Zhang, J.-M. Constitutive Rules of Cyclic Behavior of Interface Between Structure and Gravelly Soil. *Mech. Mater.* **2009**, *41*, 48–59. [CrossRef]
80. Sun, J.; Shi, G. Bounding Surface Model for Soil-structure Interface Under Cyclic Loading. *Rock Soil Mech.* **2007**, *28*, 311–314.
81. Kong, X.; Liu, J.; Zou, D.; Song, Y.; Chen, K.; Qu, Y.; Gong, J. State-of-the-art: Computational Model for Soil-interface-structure System. *Chin. J. Geotech. Eng.* **2021**, *43*, 397–405.
82. Uddin, M.; Wright, F.; Coombe, D.A. Numerical Study of Gas Evolution and Transport Behaviours in Natural Gas-Hydrate Reservoirs. *J. Can. Pet. Technol.* **2010**, *50*, 70–88. [CrossRef]
83. Hao, E.; Wei, H.; Yan, R.; Wei, C. Constitutive Model for Gas Hydrate-bearing Sediments Considering Gamage. *Chin. J. Rock Mech. Eng.* **2012**, *31*, 6.
84. Liu, X.; Flemings, P.B. Dynamic Multiphase Flow Model of Hydrate Formation in Marine Sediments. *J. Geophys. Res. Solid Earth* **2007**, *112*, B3. [CrossRef]
85. Minagawa, H.; Nishikawa, Y.; Ikeda, I.; Miyazaki, K.; Takahara, N.; Sakamoto, Y.; Komai, T.; Narita, H. Characterization of Sand Sediment by Pore Size Distribution and Permeability Using Proton Nuclear Magnetic Resonance Measurement. *J. Geophys. Res. Solid Earth* **2008**, *113*, B07210. [CrossRef]
86. Santamarina, J.C.; Dai, S.; Terzariol, M.; Jang, J.; Waite, W.F.; Winters, W.J.; Nagao, J.; Yoneda, J.; Konno, Y.; Fujii, T. Hydro-bio-geomechanical Properties of Hydrate-bearing Sediments from Nankai Trough. *Mar. Pet. Geol.* **2015**, *66*, 434–450. [CrossRef]
87. Konno, Y.; Yoneda, J.; Egawa, K.; Ito, T.; Jin, Y.; Kida, M.; Suzuki, K.; Fujii, T.; Nagao, J. Permeability of Sediment Cores from Methane Hydrate Deposit in the Eastern Nankai Trough. *Mar. Pet. Geol.* **2015**, *66*, 487–495. [CrossRef]
88. Delli, M.L.; Grozic, J. Experimental Determination of Permeability of Porous Media in the Presence of Gas Hydrates. *J. Pet. Sci. Eng.* **2014**, *120*, 1–9. [CrossRef]
89. Goel, N.; Shah, S.; Wiggins, M. Analytical Modeling of Gas Recovery from in Situ Hydrates Dissociation. *J. Pet. Sci. Eng.* **2001**, *29*, 115–127. [CrossRef]
90. Moridis, G.J.; Sloan, E.D. Gas Production Potential of Disperse Low-saturation Hydrate Accumulations in Oceanic Sediments. *Energy Convers. Manag.* **2007**, *48*, 1834–1849. [CrossRef]
91. Kurihara, M.; Ouchi, H.; Inoue, T.; Yonezawa, T.; Masuda, Y.; Dallimore, S.R.; Collett, T.S. *Analysis of the JAPEX/JNOC/GSC et al. Mallik 5L-38 Gas Hydrate Thermal-Production Test through Numerical Simulation*; Scientific Results from the Mallik 2002 Gas Hydrate Production Well Program; Geological Survey of Canada: Vancouver, BC, Canada, 2005; p. 139.
92. Liu, Z.; Yu, X. Thermo-Hydro-Mechanical-Chemical Simulation of Methane Hydrate Dissociation in Porous Media. *Geotech. Geol. Eng.* **2013**, *31*, 1681–1691. [CrossRef]
93. Kimoto, S.; Oka, F.; Fushita, T.; Fujiwaki, M. A Chemo-thermo-mechanically Coupled Numerical Simulation of the Subsurface Ground Deformations Due to Methane Hydrate Dissociation. *Comput. Geotech.* **2007**, *34*, 216–228. [CrossRef]
94. Rutqvist, J.; Moridis, G. Coupled Hydrological, Thermal and Geomechanical Analysis of Wellbore Stability in Hydrate-Bearing Sediments. In Proceedings of the Offshore Technology Conference, Houston, TX, USA, 5–8 May 2008.
95. Soga, K.; Ng, M.; Klar, A. Coupled deformation–flow Analysis for Methane Hydrate Extraction. *Géotechnique* **2010**, *60*, 765–776.
96. Kakumoto, M.; Tenma, N.; Sakamoto, Y.; Miyazakai, K.; Mori, J. Development of the Geo-Mechanical Simulation Code COTHMA. Paper presented at the Ninth ISOPE Ocean Mining Symposium, Maui, HI, USA, 19–24 June 2011.
97. Gao, Y.; Sun, B.; Zhao, X.; Wang, Z.; Yin, Z.; Wang, J. Multiphase Flow in Wellbores and Variation Laws of the Bottom Hole Pressure in Gas Hydrate Drilling. *Acta Pet. Sin.* **2012**, *33*, 6.
98. Qiu, K.; Yamamoto, K.; Birchwood, R.; Chen, Y. Well-integrity Evaluation for Methane-hydrate Production in the Deepwater Nankai Trough. *SPE Drill. Complet.* **2015**, *30*, 52–67. [CrossRef]
99. Deng, Z.; Wang, Z.; Zhao, Y.; Guo, Y.; Zhang, J.; Sun, B. Flow Assurance during Gas Hydrate Production: Hydrate Regeneration Behavior and Blockage Risk Analysis in Wellbore. In Proceedings of the Abu Dhabi International Petroleum Exhibition & Conference, Abu Dhabi, United Arab Emirate, 13–16 November 2017.
100. Moridis, G.J.; Collett, T.S.; Pooladi-Darvish, M.; Hancock, S.H.; Santamarina, J.C.; Boswell, R.; Kneafsey, T.J.; Rutqvist, J.; Reagan, M.T.; Sloan, E.D. Challenges, Uncertainties and Issues Facing Gas Production from Hydrate Deposits in Geologic Systems. *Soc. Pet. Eng.* **2010**, *14*, 76–112.
101. Li, L.; Cheng, Y.; Mei, W.; Li, Q.; Gao, L. Finite Element Simulation of Temperature Impact on Wellbore Stability of Gas-hydrate-bearing Sediments. *Nat. Gas Ind.* **2012**, *32*, 74–78.
102. Cao, Y.; Deng, J. Wellbore Stability Research of Heterogeneous Formation. *J. Appl. Sci.* **2014**, *14*, 33–39. [CrossRef]
103. Liu, M.; Jin, Y.; Lu, Y.; Chen, M.; Hou, B.; Chen, W.; Wen, X.; Yu, X. A Wellbore Stability Model for a Deviated Well in a Transversely Isotropic Formation Considering Poroelastic Effects. *Rock Mech. Rock Eng.* **2016**, *49*, 3671–3686. [CrossRef]

104. Tan, C.P.; Freij-Ayoub, R.; Clennell, M.B.; Tohidi, B.; Yang, J. Managing Wellbore Instability Risk in Gas Hydrate-Bearing Sediments. In Proceedings of the SPE Asia Pacific Oil and Gas Conference and Exhibition, Jakarta, Indonesia, 5–7 April 2007.
105. Wenke, C.; Jingen, D.; Baohua, Y.; Wei, L.; Qiang, T. Offshore wellbore Stability Analysis Based on Fully Coupled Poro-thermo-elastic Theory. *J. Geophys. Eng.* **2017**, *14*, 380–396.
106. Freij-Ayoub, R.; Tan, C.; Clennell, B.; Tohidi, B.; Yang, J. A Wellbore Stability Model for Hydrate Bearing Sediments. *J. Pet. Sci. Eng.* **2007**, *57*, 209–220. [CrossRef]
107. Yin, Y.; Cai, Y.; Chen, C.; Liu, J. Theoretical Solution of Casing Loading in Non-uniform Ground Stress Field. *Acta Pet. Sin.* **2006**, *27*, 6.
108. Wan, X. *Research on Cement Hull Mechanics of Oil and Gas Well Cementing*; Southwest Petroleum University: Chengdu, China, 2006.
109. Li, J.; Lin, C.; Yang, S.; Zhi, Y.; Chen, S. Theoretical solution of thermal stress for casing-cement-formation coupling system. *J. China Univ. Pet.* **2009**, *33*, 63–69.
110. Chu, W.; Shen, J.; Yang, Y.; Li, Y.; Gao, D. Calculation of Micro-annulus Size in Casing-cement Sheath-formation System under Continuous Internal Casing Pressure Change. *Pet. Explor. Dev.* **2015**, *42*, 379–385. [CrossRef]
111. Salehabadi, M.; Jin, M.; Yang, J.; Haghighi, H.; Ahmed, R.; Tohidi, B. Finite Element Modeling of Casing in Gas-Hydrate-Bearing Sediments. *SPE Drill. Complet.* **2009**, *24*, 545–552. [CrossRef]
112. Kim, J.; Moridis, G.J.J.; Yang, D.; Rutqvist, J. Numerical Studies on Two-Way Coupled Fluid Flow and Geomechanics in Hydrate Deposits. *SPE J.* **2012**, *17*, 485–501. [CrossRef]
113. Fereidounpour, A.; Vatani, A. An Investigation of Interaction of Drilling Fluids with Gas Hydrates in Drilling Hydrate Bearing Sediments. *J. Nat. Gas Sci. Eng.* **2014**, *20*, 422–427. [CrossRef]
114. Golmohammadi, S.M.; Nakhaee, A. A Cylindrical Model for Hydrate Dissociation near Wellbore during Drilling Operations. *J. Nat. Gas Sci. Eng.* **2015**, *27*, 1641–1648. [CrossRef]
115. Sasaki, T.; Soga, K.; Elshafie, M.Z.E.B. Simulation of Wellbore Construction in Offshore Unconsolidated Methane Hydrate-bearing formation. *J. Nat. Gas Sci. Eng.* **2018**, *60*, 312–326. [CrossRef]
116. Shengyu, J.; Guoming, C.; Xiangkun, M.; Dongdong, Y.; Yuan, Z.; Kang, L.; Yuanjiang, C. Integrity Control Analysis of Natural Gas Hydrate Production Wellbore Using System Method and Game Theory. *J. Loss Prev. Process Ind.* **2021**, *75*, 104696.
117. Chen, Z.; You, C.; Lv, T.; Li, X.; Zhang, Y.; Xu, L. Numerical simulation of the depressurization production of natural gas hydrate reservoirs by vertical well patterns in the northern South China Sea. *Natural Gas Ind.* **2020**, *8*, 177–185.
118. Chang, Y.; Huang, S.; Wang, K.; Sun, B.; Li, H.; Sun, H.; Chen, G. Study on 3D Nonlinear Coupling Wellbore-soil Model of Natural Gas Hydrate Production Test. *J. Cent. South Univ. Sci. Technol.* **2022**, *53*, 942–951.
119. Sun, J.; Ning, F.; Lei, H.; Gai, X.; Sánchez, M.; Lu, J.; Li, Y.; Liu, L.; Liu, C.; Wu, N.; et al. Wellbore Stability Analysis during Drilling through Marine Gas Hydrate-bearing Sediments in Shenhu area: A case study. *J. Pet. Sci. Eng.* **2018**, *170*, 345–367. [CrossRef]
120. Zhang, X.; Wang, S. Advances in Study of Mechanical Properties of Gas Hydrate-bearing sediments. *Open Ocean. Eng. J.* **2013**, *6*, 26–40.
121. Lu, J.; Li, D.; Liang, D.; Shi, L.; Zhou, X.; He, Y. An innovative experimental apparatus for the analysis of sand production during natural gas hydrate exploitation. *Rev. Sci. Instrum.* **2021**, *92*, 105110. [CrossRef]
122. Hiroyuki, O.; Jiro, N.; Kiyofumi, S.; Hideo, N. Experimental Analysis of Sand Production from Methane Hydrate Bearing Sediments Applying Depressurization Method. *Shigen Sozai* **2011**, *126*, 497–502.
123. Jung, J.W.; Jang, J.; Santamarina, J.C.; Tsouris, C.; Phelps, T.J.; Rawn, C.J. Gas Production from Hydrate-Bearing Sediments: The Role of Fine Particles. *Energy Fuels* **2012**, *26*, 480–487. [CrossRef]
124. Murphy, A.; Soga, K.; Yamamoto, K. A Laboratory Investigation of Sand Production Simulating the 2013 Daini-Atsumi Knoll Gas Hydrate Production Trial Using a High Pressure Plane Strain Testing Apparatus. In Proceedings of the 9th International Conferences on Gas Hydrate, Denver, CO, USA, 25 June 2017.
125. Uchida, S.; Klar, A.; Charas, Z.; Yamamoto, K. Thermo-hydro-mechanical Sand Production Model in Hydrate-bearing Sediments. In Proceedings of the EAGE International Workshop on Geomechanics and Energy—The Ground as Energy Source and Storage, Lausanne, Switzerland, 26–28 November 2013.
126. Uchida, S.; Klar, A.; Yamamoto, K. Sand Production Modeling of the 2013 Nankai Offshore Gas Production Test. In Proceedings of the 1st International Conference on Energy Geotechnics, Kiel, Germany, 29 August–1 September 2016.
127. Xu, E.; Soga, K.; Zhou, M.; Uchida, S.; Yamamoto, K. Numerical Analysis of Wellbore Behaviour during Methane Gas Recovery from Hydrate Bearing Sediments. In Proceedings of the Offshore Technology Conference, Houston, TX, USA, 5–8 May 2014.
128. Zhou, M.; Xu, E.; Soga, K.; Uchida, S.; Yamamoto, K. Numerical Study on Eastern Nankai Trough gas Hydrate Production Test. In Proceedings of the Offshore Technology Conference, Houston, TX, USA, 5–8 May 2014.
129. Ning, F.; Sun, J.; Liu, Z.; Liang, J. Prediction of Sand Production in Gas Recovery from the Shenhu Hydrate Reservoir by Depressurization. In Proceedings of the 9th International Conference on Gas Hydrate, Denver, CO, USA, 25–30 June 2017.
130. Yu, T.; Liu, Y.; Song, Y. Experimental Study on Sand Production Characteristics in Natural Gas Hydrate Deposits. In *IOP Conference Series: Earth and Environmental Science*; IOP Publishing: Bristol, UK, 2020.
131. Yan, C.; Ren, X.; Cheng, Y.; Song, B.; Li, Y.; Tian, W. Geomechanical Issues in the Exploitation of Natural Gas Hydrate. *Gondwana Res.* **2020**, *81*, 403–422. [CrossRef]
132. Zhu, H.; Xu, T.; Yuan, Y.; Xia, Y.; Xin, X. Numerical Investigation of the Natural Gas Hydrate Production Tests in the Nankai Trough by incorporating sand migration. *Appl. Energy* **2020**, *275*, 115384. [CrossRef]

133. Zhou, S.; Yang, L.; Lv, X.; Xue, K.; Zhao, J.; Liu, Y.; Yang, S. Fine Sand Migration in Hydrate-bearing Sediments and Median Grain Size Ratio Optimization of Gravel Pack. *J. Nat. Gas Sci. Eng.* **2021**, *88*, 103809. [CrossRef]
134. Hao, Y.; Liang, J.; Kong, C.; Fan, M.; Xu, H.; Yang, F.; Yang, S. Study on the Influence of Sand Production on Seepage Capacity in Natural Gas Hydrate Reservoirs. *Geofluids* **2021**, *2021*, 6647647. [CrossRef]
135. Ding, J.; Cheng, Y.; Yan, C.; Lu, C.; Li, Y.; Xue, M. Numerical Simulation on Sand Production in the Exploitation Process of Gas Hydrates Based on Skeleton Failure of Reservoirs. *J. Nat. Gas Sci. Eng.* **2021**, *94*, 104052. [CrossRef]
136. Jin, Y.; Li, Y.; Wu, N.; Yang, D. Characterization of Sand Production for Clayey-Silt Sediments Conditioned to Openhole Gravel-Packing: Experimental Observations. *SPE J.* **2021**, *26*, 3591–3608. [CrossRef]
137. Song, J.; Fu, J.; Xiong, Y.; Pang, W.; He, Y.; Liu, L.; Huang, T.; Liu, C.; Li, Y.; Li, J. State-of-the-art Brief Review on Sanding Problem of Offshore Natural Gas Hydrates Sediments. *Energy Sci. Eng.* **2021**, *10*, 253–273. [CrossRef]
138. Xiangyu, F.; Dianheng, Y.; Fulong, N.; Linjie, W.; Zhichao, L.; Yanjiang, Y.; Wenwei, X.; Hongfeng, L.; Yanlong, L.; Meng, X. Experimental Study on Sand Production and Reservoir Response of Clayey Silt Hydrate during Depressurization. *Petroleum* 2021, *in press*. [CrossRef]
139. Zhang, Y.; Wang, W.; Zhang, P.; Li, G.; Tian, S.; Lu, J.; Zhang, B. A Solution to Sand Production from Natural Gas Hydrate Deposits with Radial Wells: Combined Gravel Packing and Sand Screen. *J. Mar. Sci. Eng.* **2022**, *10*, 71. [CrossRef]
140. Chuanliang, Y.; Yang, L.; Yuanfang, C.; Jia, W.; Wanqing, T.; Shuxia, L.; Zhiyuan, W. Multifield Coupling Mechanism in Formations around a Wellbore during the Exploitation of Methane Hydrate with CO_2 Replacement. *Energy* **2022**, *245*, 123283.
141. Ya-Ting, X.; Yi, W.; Xiao-Sen, L.; Xiao-Yan, L.; Gang, L.; Fu-Cheng, D. Experimental Research on the Influence of Particle Size on Sand Production during Gas Hydrate Dissociation via Depressurization. *Energy Fuels* **2022**, *36*, 10541–10551.
142. Zhang, P.; Zhou, Y.; Liu, B.; Deng, W. Multiphase Flow Model Coupled with Fine Particle Migration for Applications in Offshore Gas Hydrate Extraction. *J. Nat. Gas Sci. Eng.* **2022**, *102*, 104586. [CrossRef]
143. Haiyan, Z.; Xuanhe, T.; Fengshou, Z.; David, M.J. Mechanical Behavior of Methane–Hydrate–Bearing Sand with Nonlinear Constitutive Model. *Arab. J. Sci. Eng.* **2022**, *47*, 12141–12167.
144. Jiping, D.; Yuanfang, C.; Chuanliang, Y. Research on Sand Control Effect and Micro-plugging Mechanism of Sand Control Medium in the Development of Natural Gas Hydrate Reservoir. *J. Pet. Sci. Eng.* **2022**, *215*, 110703.
145. Xiao-Yan, L.; Heng-Qi, H.; Yi, W.; Xiao-Sen, L. Experimental Study of Gas-liquid-sand Production Behaviors during Gas Hydrates Dissociation with Sand Control Screen. *Energy* **2022**, *254*, 124414.
146. Bin, G.; Ruiqi, Z.; Tianwei, S.; Yujing, J.; Naser, G.; Yanlong, L.; Shanilka, G.F.; Madusanka, N.J. Coupling Model of Submarine Deformation Response Prediction during Methane Hydrate Exploitation. *Energy Fuels* **2022**, *36*, 6785–6809.
147. Fang, X.; Ning, F.; Wang, L.; Liu, Z.; Lu, H.; Yu, Y.; Li, Y.; Sun, J.; Shi, H.; Zhao, Y.; et al. Dynamic Coupling Responses and Sand Production Behavior of Gas Hydrate-bearing Sediments during Depressurization: An Experimental Study. *J. Pet. Sci. Eng.* **2021**, *201*, 108506. [CrossRef]
148. Wang, Y.; Gao, D.; Fang, J. Finite Element Analysis of Deepwater Conductor Bearing Capacity to Analyze the Subsea Wellhead Stability with Consideration of Contact Interface Models between Pile and Soil. *J. Pet. Sci. Eng.* **2014**, *126*, 48–54. [CrossRef]
149. Li, J.; Chang, Y.; Xiu, Z.; Liu, H.; Xue, A.; Chen, G.; Xu, L.; Sheng, L. A Local Stress-strain Approach for Fatigue Damage Prediction of Subsea Wellhead System Based on Semi-decoupled Model. *Appl. Ocean. Res.* **2020**, *102*, 102306. [CrossRef]
150. Yan, W.; Chen, Z.-J.; Deng, J.-G.; Zhu, H.-Y.; Deng, F.-C.; Liu, Z.-L. Numerical Method for Subsea Wellhead Stability Analysis in Deepwater Drilling. *Ocean. Eng.* **2015**, *98*, 50–56. [CrossRef]
151. Adamiec-Wójcik, I.; Wojciech, S. Application of The Finite Segment Method to Stabilisation of the Force in A Riser Connection with A Wellhead. *Nonlinear Dyn.* **2018**, *93*, 1853–1874. [CrossRef]
152. Li, W.; Gao, D.; Yang, J.; Hu, Z.; Abimbola, F. Subsea Wellhead Stability Study of Composite Casing for Deepwater Drilling. *Ocean. Eng.* **2020**, *214*, 107780. [CrossRef]
153. Xu, Y.; Guan, Z.; Jin, Y.; Liu, Y.; Sun, Y.; Zhang, B.; Sheng, Y. Risk Assessment Method of Subsea Wellhead Instability in Consideration of Uncertain Factors in Deepwater Drilling. *Arab. J. Sci. Eng.* **2017**, *43*, 2659–2672. [CrossRef]
154. Su, K.; Guang, Z.; Su, Y. Mechanical Stability Analysis of Subsea Wellhead for Deepwater Drilling. *Oil Drill. Prod. Technol.* **2008**, *30*, 1–4, 15.
155. Guan, D.; Yan, W. Stability Analysis of Underwater Wellhead in Deepwater Drilling. *China Pet. Mach.* **2012**, *40*, 85–89.
156. Zhang, J.; Pang, D.; Xu, J.; Hu, J.; Cao, Y.; Chen, Q. Wellhead stability analysis of surface casing running for deepwater drilling. *Oil Drill. Prod. Technol.* **2018**, *40* (Suppl. S1), 101–103.
157. Zhou, Y.; Zhou, B.; Li, L.; Wang, K.; Wang, J.; Yang, X. Influence of the Top Tension of Riser on the Stability of Subsea Wellhead System. *Oil Drill. Prod. Technol.* **2018**, *40* (Suppl. S1), 98–100.
158. Yang, J.; Li, W.; Hu, Z.; Yin, Q.; Li, S. Research Progresses on Subsea Wellhead Stability of Deep Water Drilling. *China Offshore Oil Gas* **2020**, *32* (Suppl. S1), 98–100.
159. Wu, Y.; Xing, X.; Pang, Z.; Huang, Z. Research and Application of Key Technologies of Integrated Drilling and Completion for Offshore Exploration and Development. *China Offshore Oil Gas* **2022**, *34*, 128–133.
160. Li, Q.; Cheng, Y.; Zhang, H.; Yan, C.; Liu, Y. Simulating the Effect of Hydrate Dissociation on Wellhead Stability during Oil and Gas Development in Deepwater. *J. Ocean. Univ. China* **2018**, *17*, 35–45. [CrossRef]
161. Yang, L.; Wang, J. Effect of Depressurized Hydrate on Soil Layer Around Wellhead. In *IOP Conference Series: Earth and Environmental Science*; IOP Publishing: Bristol, UK, 2020.

162. Li, P.; Yang, J.; Lu, B.; Ke, K.; Wang, L.; Chen, K. Research on Stratum Settlement and Wellhead Stability in Deep Water during Hydrate Production TestingChinese Full Text. *Pet. Drill. Tech.* **2020**, *48*, 61–68.
163. Su, K. A Device for Preventing the Instability of Underwater Wellhead in Deep Water. Drilling. Patent CN202451101U, 26 September 2012.
164. Su, K.; Yang, J.; Butt, S. An Innovative Device to Enhance Conductor Bearing Capacity in Deepwater Drilling Operations. *J. Offshore Mech. Arct. Eng.* **2018**, *140*, 011302. [CrossRef]
165. Kan, C.; Yang, J.; Yu, X.; Dong, T.; Wu, X.; Liu, M.; Li, C.; Zhang, C.; Fu, J. Load Bearing Characteristics Study on Novel Deepwater Composite Drilling Conductor by Simulation and Experimental Methods. *J. Pet. Sci. Eng.* **2018**, *171*, 289–301. [CrossRef]
166. Su, K.; Guang, Z.; Wei, L.; Liu, Y. Analysis on Subsea Wellhead Stability of Surface BOP Drilling System in Deepwater Operations. *China Offshore Oil Gas* **2009**, *21*, 180–185.
167. Dib, M.W.; Lou, J.; Zhu, L.; Bassey, M. SBOP Drilling Enables Efficient Drilling in Extreme Water Depths. In Proceedings of the Offshore Technology Conference, Houston, TX, USA, 4–7 May 2009.
168. Cheng, G.; Duan, M.; Ye, M.; Li, M.; Sun, C.; Wang, F. Bearing Capacity of Suction Piles Used in Deep Water Subsea System. *Oil Field Equip.* **2013**, *42*, 46–50.
169. Sivertsen, T.; Strand, H. New Well Foundation Concept, as Used at a Norwegian Sea well. In Proceedings of the SPE Arctic and Extreme Environments Conference and Exhibition, Moscow, Russia, 18–20 October 2011.
170. Qin, Y.; Liu, K.; Chen, G.; Zhang, A.; Zhu, J.; Xia, K. Negative Pressure Analysis for the Penetration Installation of Conductor Suction Anchor in Marine Hydrate Reservoirs. *Oil Drill. Prod. Technol.* **2021**, *43*, 737–743.
171. Gong, Z.; Zhang, L.; Cheng, H.; Liu, Y.; Ren, S. The Influence of Subsea Natural Gas Hydrate Dissociation on the Safety of Offshore Drilling. *Pet. Drill. Tech.* **2015**, *43*, 19–24.
172. Li, W.; Gao, D.; Yang, J. Challenges and Prospect of the Drilling and Completion Technologies Used for the Natural Gas Hydrate Reservoirs in Sea Areas. *Oil Drill. Prod. Technol.* **2019**, *41*, 681–689.
173. Zhou, S.; Chen, W.; Li, Q.; Chen, J.; Shi, H. Research on the Solid Fluidization Well Testing and Production for Shallow Non-diagenetic Natural Gas Hydrate in Deep Water Area. *China Offshore Oil Gas* **2017**, *29*, 1–8.
174. Zhou, S.; Chen, W.; Li, Q.; Zhou, J.; Shi, H. Thinking and Suggestions on Research Direction of Natural Gas Hydrate Development. *China Offshore Oil Gas* **2019**, *31*, 1–8.
175. Wang, B.; Huo, P.; Luo, T.; Fan, Z.; Liu, F.; Xiao, B.; Yang, M.; Zhao, J.; Song, Y. Analysis of the Physical Properties of Hydrate Sediments Recovered from the Pearl River Mouth Basin in the South China Sea: Preliminary Investigation for Gas Hydrate Exploitation. *Energies* **2017**, *10*, 531. [CrossRef]